



University of
Massachusetts
Amherst

Two Approaches to the Study of the Mechanism of the Transition Process from Initiation to Elongation in T7 Rna Polymerase

Item Type	Thesis (Open Access)
Authors	Redhu, Shiv K
DOI	10.7275/600269
Download date	2026-04-21 22:30:27
Link to Item	https://hdl.handle.net/20.500.14394/45229

**TWO APPROACHES TO THE STUDY OF THE MECHANISM OF THE
TRANSITION PROCESS FROM INITIATION TO ELONGATION IN T7 RNA
POLYMERASE**

A Thesis Presented

By

SHIV KUMAR REDHU

**Submitted to the Graduate School of the
University of Massachusetts Amherst in partial fulfillment
of the requirements for the degree of**

MASTER OF SCIENCE

September 2008

Chemistry

© Copyright by Shiv Kumar Redhu 2008

All Rights Reserved

TWO APPROACHES TO THE STUDY OF THE MECHANISM OF THE TRANSITION
PROCESS FROM INITIATION TO ELONGATION IN T7 RNA POLYMERASE

A Thesis Presented

by

SHIV KUMAR REDHU

Approved as to style and content by:

Craig T. Martin, Chair

Richard W. Vachet, Member

Karsten W. Theis, Member

Bret Jackson, Department Head
Department of Chemistry

DEDICATION

To my parents, younger sister, and brothers.

ACKNOWLEDGEMENTS

First, my heartfelt thanks to my Mom and Dad, who always have been my strength at every stage of my life. Love to my younger sister and brothers. Without their (my family) endless love, encouragement, and support, I would have perished a long before in my journey of life. I really admire them and love them; they are my “Inspiration”.

I thank Professor Craig Martin for his guidance, patience, and financial support throughout my stay in the department. He is a great mentor and a very nice person. I have learned a lot from him.

I thank Professors Richard Vachet, and Karsten Theis for being members of my committee and their valuable suggestions, instructions, and advices.

I thank all my past and present labmates. All of you made my stay in the lab a pleasant one. Thanks to Peng Gong for helpful discussions, supports, and instructions to get me started on my research. Thanks to Rosemary Turingan for encouragement and valuable discussions while working together. Thanks to Metewo Selase Enuameh, Yi Zhou, Xiaoqing Liu, and Ankit Vahiya for any kind of help. I wish all of you a great scientific career. Special thanks to Selase for being a good friend. Your friendship will always be remembered.

I thank Dan Fowler and Fe Consolacion for being good friends, and I also want to extend my gratitude to Prof. Robert Weis group members for letting me use their lab instruments. Thanks to Robert Sabola for helping our whole group with instruments problems.

Finally, I would like to thank the group of undergraduates that I had opportunity to work with; Bruno Karam, Katarina Anderson, and Yadilette Rivera. I really enjoyed the time spent with you all. My heartfelt gratitude to all others whose names I did not mention, but who contributed in any form towards the successful completion of the thesis.

ABSTRACT

TWO APPROACHES TO THE STUDY OF THE MECHANISM OF THE
TRANSITION PROCESS FROM INITIATION TO ELONGATION IN T7 RNA
POLYMERASE

SEPTEMBER 2008

SHIV KUMAR REDHU

B.S., KURUKSHETRA UNIVERSITY

M.S., PANJAB UNIVERSITY

M.S., UNIVERSITY OF MASSACHUSETTS AMHERST

DIRECTED BY: PROFESSOR CRAIG T. MARTIN

Abortive transcription, the premature release of short transcripts 2-8 bases in length, is a unique feature of transcription, accompanying the transition from initiation to elongation in all RNA polymerases. However, the mechanism of the instability of abortive cycling in RNA polymerase is not been well understood. The current study focuses on major factors that relate to the stability of initially transcribing abortive complexes in T7 RNA polymerase. Building on previous studies that reveal that collapse of the DNA from the downstream end of the bubble is a major contributor to the characteristic instability of abortive complexes, we now propose that collapse contributes to the release of abortive products in the presence of all four NTPs. Specifically, we propose that stabilizing initially transcribing complexes against downstream bubble collapse will allow these complexes to escape better to full run elongation. This study

will provide important mechanistic insight, but will also be valuable for the production of high quantities of RNA from highly abortive DNA sequences.

We have recently proposed a new model for the transition from initiation to elongation in T7 RNA polymerase. DNA-to-DNA FRET measurements have allowed mapping the changes that occur before promoter release. To observe the movements of the rotating domain after promoter release requires protein labeling. We are developing a new technique of affinity directed site specific labeling of the protein. We have also begun to explore an intein mediated strategy for direct labeling of T7 RNA polymerase.

TABLE OF CONTENTS

	Page
ACKNOWLEDGEMENTS	v
ABSTRACT	vii
LIST OF FIGURES	xi
CHAPTER	1
1. INTRODUCTION	1
1.1 General Background:	1
1.2 T7 RNA polymerase:	2
1.2.1 Promoter binding and de novo initiation:	4
1.2.2 Transition toward elongation and abortive cycling:	6
1.3 Summary	13
1.4 References:	14
2. ABORTIVE CYCLING IN T7 RNA POLYMERASE.....	19
2.1 Introduction:	19
2.2 An integrated model for abortive cycling:	23
2.3 Results:	26
2.3.1 Instability of the Abortive Complexes due to the Transcription Bubble Collapse form the Downstream End	26
2.3.2 Effect of NTP concentration on the abortive profile of mismatched DNA constructs	29
2.3.3 Characterization of abortive complexes in runoff transcription reaction:	31
2.4 Materials and Method	37
2.4.1 Protein expression and purification	37
2.4.2 Oligonucleotide synthesis and purification	37
2.4.3 Double stranded or partially single stranded DNA construction	38
2.4.4 Transcription assays	38
2.5 References:	39

3. SITE SPECIFIC LABELING OF T7 RNA POLYMERASE	45
3.1 Fluorescence Resonance Energy Transfer Overview:	45
3.2. SITE-SPECIFIC LABELING OF T7 RNA POLYMERASE:.....	48
3.2.1. The strategy of site specific labeling:	49
3.3 Preliminary Results:.....	54
3.4 An alternate route of site-specific protein labeling:.....	56
3.4.1 Expressed Protein Ligation:.....	57
3.4.2 Protein <i>trans</i> -splicing:.....	60
3.3 Scheme of making recombinant T7 RNA polymerase	62
3.4 Materials and Methods:.....	65
3.4.1 Construction and purification of the mutant (A94C) & WT T7 RNA polymerase	65
3.4.2 Synthesis and purification of oligonucleotides	66
3.4.3 Synthesis and fluorescent probe labeling of DNA.....	67
3.4.4 Determining corrected single-stranded DNA concentration.....	69
3.4.5 Preparation of duplex DNA	70
3.4.6 Binding and cross-linked complex formation.....	72
3.4.7 Streptavidin-bead pull down assay	73
3.4.8 Transcription and sink-challenge assay	74
3.5 References:.....	76
BIBLIOGRAPHY	83

LIST OF FIGURES

Figure	Page
1.1: Promoter-binding interface of T7 RNA polymerase	5
1.2: Comparison of the initiation and the elongation complex structures	9
2.1: A model for abortive cycling	25
2.2: Transcription profile of lac sequence.....	28
2.3: P266L lies in a region that undergoes substantial structural change	42
2.4: Effect of NTP concentrations on abortive profiles	30
2.5: Comparison of mismatches and nicks modifications	32
2.6: Abortive profile of mismatched DNA constructs	34
3.1: Schematic presentation of FRET between donor and acceptor.	47
3.4: DNA construct used for labeling protein.....	49
3.5: Scheme for site-specifically labeling the protein.....	50
3.6: DNA constructs used for bead pull down assay	52
3.7: Structures of 6-carboxyfluorescein phosphoramidite and the photocleavable (PC) spacer phosphoramidite (Glen Research).....	53
3.8. The transcription assay on wild-type (WT) and A94C mutant T7 RNA polymerase complexes to assess the formation of crosslinked complexes.....	54
3.9: Transcribing complexes (Correct crosslinked; resistant to sink) after first bead pull down assay.	55
3.10: The principle of expressed protein ligation	71
3.11: Sequential ligation strategy.....	72
3.12: Principle of protein <i>trans</i> -splicing (PTS).....	61
3.13: Scheme of recombinant protein α -thioesters and expressed protein ligation..	63
3.14: A) Schematic presentation of engineering restriction site in pBH161 plasmid and insertion of the fragments of interest in pTWIN vector, B) schematic presentation of protein ligation process to yield recombinant protein.....	64

3.15: Schematic presentation of sink challenge assay.75

CHAPTER 1

INTRODUCTION

1.1 General Background:

Transcription is the primary regulatory process used by cells, tissues, and organisms to facilitate and control the complex programmes of gene expression, cellular metabolism, and organ and tissue development. Many aberrant events that lead to the development of tumors and cancer also depend on transcription. Transcription, the synthesis of RNA on a DNA template, is a cyclic process performed by the highly processive, DNA dependent RNA polymerase (RNAP). The polymerases can be differentiated based on their complexity, whether they are made up of single subunit consisting of single polypeptide chain, or they are more complex system with multiple subunits. Initiation and regulation of transcription in multi-subunits polymerases often require assemblies of different protein subunits and multiple cofactors (Borukhov et al, 2005; Ebright, 2000; Schroeder & deHaseh, 2005). This complex assembly process of multi-subunit RNA polymerases poses certain restrictions in their isolation and purification, which renders them difficult to study mechanistically.

The bacteriophage T7, a virus which infects most strains of E. coli, is useful to molecular biologists because it has a very strong promoter specificity which directs transcription of its gene by the phage T7 RNA polymerase. The RNA polymerase from bacteriophage T7 along with RNA polymerases from bacteriophages T3, SP6, and K11, the mitochondrial nuclearly encoded chloroplast RNA polymerases, and the N4 virion RNA polymerase constitute one family of RNA polymerases (RNAPs).

1.2 T7 RNA polymerase:

T7 RNA polymerase is a prototype of single subunit RNA polymerases, and it has been highly attractive as a model for the mechanistic studies of the different phases of transcription and RNA synthesis over decades. Despite structural differences, the 99-KDa single subunit RNA polymerase from bacteriophage T7 (T7 RNAP) and the multisubunit cellular RNAPs share numerous functional characteristics. T7 RNAP carries out all of the same basic steps in the transcription cycle as the multisubunit RNAPs without the need for auxiliary factors (Cermakian et al, 1996; Jaehning, 1993). The crystal structures of T7 RNAP in an initiation complex and elongation complex have been solved to a resolution of 2.4 Å and 2.1 Å respectively (Cheetham et al, 1999; Cheetham & Steitz, 1999; Tahirov et al, 2002; Temiakov et al, 2004; Yin & Steitz, 2002; Yin & Steitz, 2004). Both crystal structures provide a great deal of information about mechanistic and structural aspects of this enzyme and have enhanced our knowledgebase of transcription by all RNA polymerases. During transcription initiation, RNAPs recognize specific promoter sequences in the DNA, melt open a duplex DNA region around the transcription start site, catalyze the formation of phosphodiester bonds *de novo*, and continue growing an RNA transcript using ribonucleoside triphosphates (NTPs) as substrates. The initially transcribing complex, which retains promoter contacts, is usually unstable, characterized by the rapid release of short transcripts 2-8 nucleotides in length. The cyclic process including initiation and the following release of short transcripts is termed abortive cycling or abortive initiation and is one of the unique features of transcription (Carpousis & Gralla, 1980; Martin et al, 1988; Milligan et al, 1987). After synthesis of about 8-10 bases, RNA polymerases escape from abortive cycling, losing the sequence-specific

contacts to the promoter DNA and forming a stable elongation complex (Cai & Luse, 1987; Carpousis & Gralla, 1985; Ikeda & Richardson, 1986). The elongation complex is highly processive and capable of synthesizing thousands of bases until RNA polymerase dissociates after reaching specific termination sequences in the DNA and/or encountering specific termination factors.

The single subunit T7 RNA polymerase has 883 amino acid residues a molecular weight of 99 KDa and a pI of 6.79. T7 RNA polymerase consists of two distinct functional domains, a N-terminal domain and a C-terminal domain, which have different functions in transcription. The amino acid residues from 1-266 comprise the N-terminal domain, and this domain is highly specific for transcription, as it is primarily involved in the promoter recognition and product displacement from the template strand (detailed below) during the process of transcription. The remaining amino acid residues from 267-283 comprise the C-terminal domain, and this domain carries the active site and is structurally very similar to the other nucleotide polymerases: for example members of the Pol I and Pol α DNA polymerase families, and human immunodeficiency virus type 1 (HIV-1) reverse transcriptase (Hansen et al, 1997; McAllister, 1997; Sousa et al, 1993; Steitz, 1999). The C-terminal domain of T7 RNA polymerase bears a resemblance to a cupped right hand with thumb and finger subdomains mounting on each side of a palm subdomain (Kohlstaedt et al, 1992), as that of the other nucleotide polymerases.

The crystal structures of T7 RNA polymerase involving a free enzyme (Sousa et al, 1993), a complex with T7 lysozyme, which is the only natural inhibitor of T7 RNA polymerase (Jeruzalmi & Steitz, 1998), an enzyme-promoter DNA binary complex (Cheetham et al, 1999), an initiation complex with a 3 base transcript (Cheetham &

Steitz, 1999), and several elongation complexes obtained from a promoter-independent method (Tahirov et al, 2002; Temiakov et al, 2004; Yin & Steitz, 2002; Yin & Steitz, 2004) have provided deep understanding and helped biochemical and biophysical studies of the T7 RNA polymerase system.

1.2.1 Promoter binding and de novo initiation:

T7 RNA polymerase recognizes a 23 base pair consensus promoter sequence extending from position -17 to +6 (Dunn & Studier, 1983) and can be differentiated into various recognition elements or regions.

The promoter binding region of T7 RNA polymerase makes sequence specific contacts with the -17 to -5 recognition element, which lies upstream of the transcription start site +1. These promoter contacts are supposed to be maintained, at least partially, up to translational positions +7 and +8 (Briebe & Sousa, 2001a; Gong et al, 2004; Ikeda & Richardson, 1986; Place et al, 1999). The interface between the promoter-binding region of the RNA polymerase and the recognition element is very alike in the structure of promoter DNA binary complex and the initiation complex with a 3mer RNA (Cheetham et al, 1999; Cheetham & Steitz, 1999). The primary features of the interface (figure 1.1) are illustrated here using the crystal structure of the initiation complex with a 3mer RNA transcript. There are three different elements of T7 RNA polymerase which interact specifically with the promoter. First, the AT rich recognition loop (residues 93-101) interacts with the -17 to -13 promoter region through the minor groove; second, the specificity loop (residues 738-769) reads out the bases around position -9 through the major groove; third, the intercalating hairpin (residues 230-245) inserts into the two DNA

strands around position -4, and most likely serves to retain the upstream end of the initially melted bubble at initiation (Briebe & Sousa, 2001b; Stano & Patel, 2002). All of these contacts seem to be responsible for preserving the intact reading of the recognition element, since out of the 13 base pairs, only 3 (at positions -17, -13, and -12) base pair substitutions can be generally tolerated with other base pairs (Imburgio et al, 2000). Although it has been proposed that the promoter contacts with the specificity loop and the intercalating hairpin may be lost earlier than that with the AT-rich recognition loop (Place et al, 1999), we favor a model in which the release of promoter contacts are accompanied by a coincident loss of all three contacts.

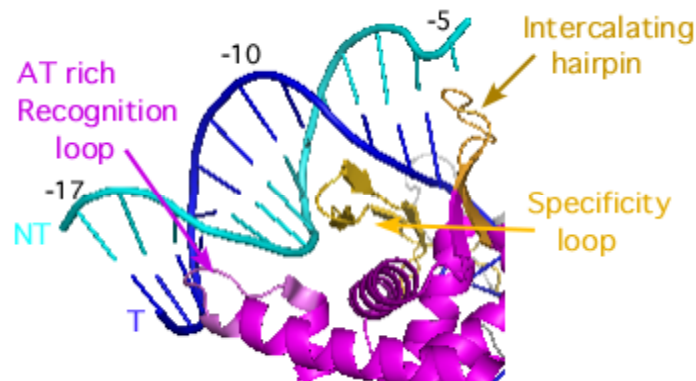


Figure 1.1: Promoter-binding interface of T7 RNA polymerase

The figure is adapted from the crystal structure of the initiation complex with a 3 base RNA (Cheetham & Steitz, 1999) with three polymerase regions interacting with the -17 to -5 recognition element. Color codes: Nontemplate strand (NT) – cyan; template strand (T) – blue; AT rich recognition loop – violet; specificity loop – gold; intercalating hairpin – coral.

The TATA (-4 to -1) element and a polymerase region called motif B (residues 614-664) supposedly facilitate melting of the initial transcription bubble, which extends from position -4 to +3 at upstream end and downstream end respectively (Cheetham & Steitz, 1999; McAllister, 1993; Újvári & Martin, 1996). T7 RNA polymerase containing mutations in the motif B region (residues 614-664) does not transcribe double stranded

promoter DNA. Rather it transcribes on partially single stranded promoter DNA (pss DNA). This finding confirms that motif B is likely involved in melting of the initially melted transcription bubble.

There are 17 T7 promoters, and 13 out of 17 promoters have cytosines (C) at position +1 and /or +2 in the template strand, which is/are supposed to be optimized for the efficient *de novo* initiation. Cs in the template strand at these positions will encode Gs in the transcript (Dunn & Studier, 1983), suggesting that GTP substrate is highly preferred by the RNA polymerase for the formation of first phosphodiester bond. Another concept related to the initially transcribing sequence from position +1 to +6 is the level of abortive products. The relationships of the level of abortive products with initially transcribing sequence have been studied by comparing endogenous and exogenous T7 promoter sequences (Guillerez et al, 2005; Lopez et al, 1997; Muller et al, 1988).

1.2.2 Transition toward elongation and abortive cycling:

Several groups have characterized abortive cycling in T7 RNA polymerase (Ling et al, 1989; Milligan et al, 1987; Muller et al, 1988). The most common conclusions that were made from these studies include: first, most of the sequences produce high levels of 6 – 8 base long abortive products; second, the more the number of Us in the transcript, more the abortive products released. There is also another class of released transcript of about 11 – 13 bases in length which are relatively lower level than abortive products, known as dead end product (Gong et al, 2004; Jia & Patel, 1997; Jiang et al, 2001; Martin et al, 1988). The release mechanism of these transcripts seems to be position dependent

rather than sequence dependent. Therefore, we are counting abortive products only up to eight bases.

The initiation promoter bound complex crystal structure of T7 RNA polymerase has no or little change in overall conformation with and without a trinucleotide transcript (Cheetham et al, 1999; Cheetham & Steitz, 1999). This shows that the release of 2-3mer products does not depend on the intrinsic stability of the RNA polymerase. The instability of the DNA-RNA hybrid seems to be an acceptable explanation for the release of these (2-3mer) abortive transcripts. Nevertheless, the reincorporation of these products complicates their analysis; for example the level of these products does not increase with time, shows no sequence dependence (Moroney & Piccirilli, 1991) and, the effect of protein and promoter DNA mutations. The scrutinized analysis of the crystal structures of T7 RNA polymerase also suggests that translocation of polymerase further down position +3 is more likely accompanied by the collision of the transcript into the N-terminal domain's helix, which induces a series of conformational changes in the polymerase and the reorganization of the whole complex into a more stable conformation i.e. elongation conformation. The biochemical and biophysical evidence that bolster our understanding of how and when these changes occur along with the comparison of polymerase initiation complex and elongation complex crystal structures (Cheetham & Steitz, 1999; Yin & Steitz, 2002) will be discussed further in this chapter.

T7 RNA polymerase undergoes a huge structural reorganization from initiation to elongation. These dramatic changes are represented in figure 1.2. As evidenced from the crystal structures, an essential promoter enzyme-binding interface in the initiation complex is disrupted in the elongation complex, as the specificity loop moved away from

the intercalating hairpin and the AT-rich recognition loop (Tahirov et al, 2002; Yin & Steitz, 2002). The RNA:DNA hybrid grows up to a length of 7-8 basepairs (fig. 1.2 and (Tahirov et al, 2002)), which is the observed length of hybrid in the elongation complex and is consistent with the earlier footprinting and fluorescence studies data (Huang & Sousa, 2000; Liu & Martin, 2001a). The growing RNA transcript establishes contacts with the newly formed RNA exit channel (Yin & Steitz, 2002). The refolding loop (residues 153- 203) plays an important role in the formation of the exit channel and in particular, the region from amino acid 170 to 180 seems very critical in the processivity of the elongation complex, as proteolytic cleavage at residue 172 or 179 diminishes the production of long RNA transcripts (Muller et al, 1988).

The N-terminal domain of T7 RNA polymerase undergoes a dramatic structural reorganization from initiation to elongation. There is little change in the C-terminal domain of the polymerase. There are several subdomains in the N-terminal domain of the polymerase that undergo structural reorganization in going from initiation to elongation. First, residues 43-71 form a helical structure that also form a part of putative upstream DNA binding cleft and the hybrid-binding domain in the elongation complex (Tahirov et al, 2002; Yin & Steitz, 2002). Second, the core subdomain or the rigid body subdomain (residues 73-152 and 204-258) supposedly stays intact in the transition process but undergoes a rigid body motion, which includes a translational movement of more than 20 Å and a rotational movement of 140° relative to its original position. The triggering or initial driving force for this core subdomain movement is almost certainly the expected steric clash between this rigid body subdomain and the growing hybrid (Tahirov et al, 2002; Yin & Steitz, 2002). Third, the refolding loop undergoes a huge structural

remodeling during the transition process and moves over 70 Å relative to the stable intact C-terminal domain. This structural remodeling of the refolding loop completes the formation of RNA exit channel and the polymerase enters into a stable elongation phase (Tahirov et al, 2002; Yin & Steitz, 2002). Two small conformational changes have been also observed in the C-terminal domain: (i) the extended specificity loop becomes less extended and interacts with RNA in the RNA exit channel and, (ii) a rotation of about 15° in the flexible thumb subdomain (residues 326-411) relative to the remaining C-terminal domain (Tahirov et al, 2002; Yin & Steitz, 2002).

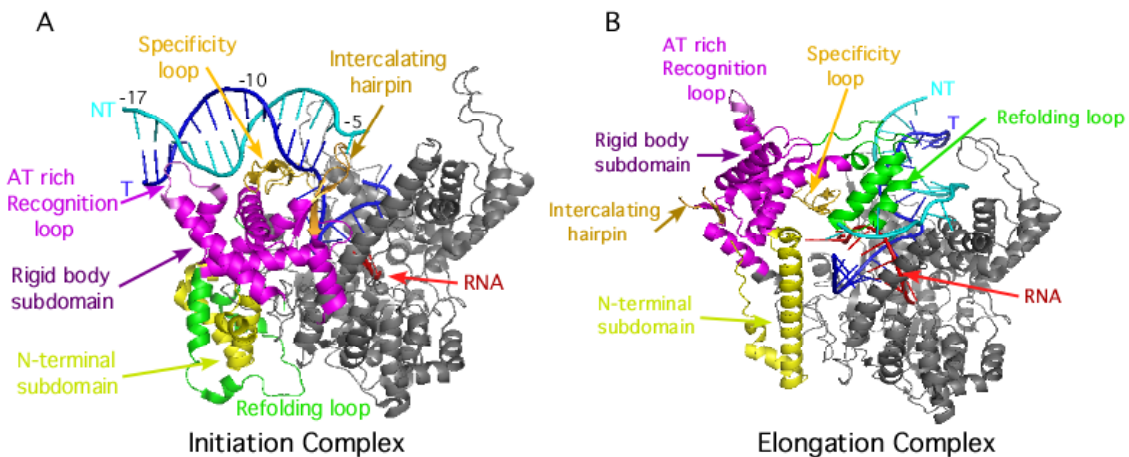


Figure 1.2: Comparison of the initiation and the elongation complex structures

The initiation complex with 3 base transcript (A) (Cheetham and Steitz, 1999) is compared with the elongation complex (B) (Yin and Steitz, 2002). Color codes: RNA – red; N-terminal subdomain – yellow; rigid body subdomain – magenta; refolding loop – green; Nontemplate strand (NT) – cyan; template strand (T) – blue; AT rich recognition loop – violet; specificity loop – gold; intercalating hairpin - coral.

Following is the elucidation of the transition process into 3 phases. The synthesis of first 2-3 bases forms the first phase of this process. The 2-3 bases of RNA can easily be accommodated in the active site without undergoing any structural modification, as

evidenced by crystal structure. The main reason for the instability of these complexes is the intrinsic instability of the short RNA:DNA hybrid.

The second phase corresponds to a series of intermediate stages during the translocation of the polymerase from position +4 to +8. As complexes are still not in the final stable elongation mode, the overall stability of these complexes is still low. A series of structural reorganizations takes place during this translocation. The retention of promoter contacts at these intermediate stages most likely plays dual roles. On one hand, it restricts the further conformational changes toward elongation by providing topological constraints, which leads to the instability of these complexes. On the other hand, it may also serve to hold the polymerase and DNA together until the RNA:DNA hybrid reaches the minimum sufficient stable length i.e. when the hybrid reaches 8 base pairs, which is stable enough to allow the system to undergo a huge dramatic structural reorganization towards elongation, after the loss of promoter contacts (promoter release).

Recently many characterizations have been carried out to study these intermediate stages. A mutation of one residue in the rigid-body subdomain (E148A) yields much higher levels of 5-6mer abortive products as compared to wild type enzyme (He et al, 1997). This study suggests that the region of the rigid-body subdomain where the mutation is located possibly takes part in establishing new interactions as this domain moves to its intermediary locations. In other study, a double mutant enzyme (D660C - R379C), in which a salt bridge was disrupted between the thumb subdomain and one of the finger subdomains, also yields much higher levels of 4-5mer abortive products (Mukherjee et al, 2003), suggesting that the thumb-finger interactions at these stages are an overall stabilizing factor.

The direct evidence for the relative movement of the N-terminal and the C-terminal domains during this transition is shown in more recent studies with engineered disulfide bonds between the two domains. An engineered disulfide linkage between the rigid-body subdomain (D147C) and the C-terminal domain (R292C) blocks transcription mainly at positions +5 to +6 bases (Ma et al, 2005) without any full-length runoff product. With the same rationale, another crosslink was done between the rigid-body subdomain (S128C) and the thumb subdomain (S393C), which also blocks transcription beyond positions +7 to +8 (Guo et al, 2005). That the crosslink allows transcription to +7 to +8 suggests a relative high flexibility in the thumb subdomain (Sousa et al, 1994). Both the above mentioned mutant enzymes do not produce longer products, suggesting that it requires a larger movement of these two domains of the protein to enter into the elongation phase. This study was further elaborated by another crosslink between the rigid-body subdomain (K206C) and the specificity loop (N764C). This mutant protein produces higher levels of 13-19 mer products and is not able to block initial transcription. DNase 1 footprinting data also suggest an impairment in promoter release. That is because the rigid-body subdomain and the specificity loops are the components of the promoter-binding platform of the polymerase and the crosslinking secures the integrity of the platform. These results along with the work of (Esposito & Martin, 2004b) suggest that the polymerase can synthesize long products without complete release of the promoter contacts.

An additional phase of the transition corresponds to translocation through position +9 to +13. This phase occurs due to the lack of promoter release (which is supposed to happen at position +8 to +10), yields a complex in which RNA is not properly dissociated. During this phase, premature release of 11-13mer products occurs mainly

due to insufficient level of stability in these complexes. The increase in their levels has been observed when the nontemplate strand downstream of position -5 is not present (Jia & Patel, 1997; Jiang et al, 2001). The same type of observation has also been made when an engineered disulfide bond between the -17 template base and A94C residue in the AT rich recognition loop of the polymerase facilitates the retention of promoter contacts (Esposito & Martin, 2004b; Gopal et al, 1999). The third phase is a very critical phase because several events occur simultaneously at this stage of the transition process. The following events take place at this stage: (i) collapse of transcription bubble from the upstream end, (ii) complete loss of promoter contacts, and (iii) the initial displacement of the 5' end of the nascent RNA transcript into RNA exit channel from DNA: RNA hybrid.

The intercalating hairpin is an important component of the promoter-binding interface (Briebe & Sousa, 2001b; Cheetham et al, 1999; Stano & Patel, 2002). It functions in the maintenance of the upstream edge of the transcription bubble. As suggested by various studies, initial transcription bubble collapse and the loss of promoter contacts are likely energetically coupled and may occur in a coincident fashion. The supporting evidence for this comes from a fluorescence study from our group, which shows that the upstream edge of the bubble begins to collapse only after translocational position +8 (Liu & Martin, 2002). Many studies suggest the retention of promoter contacts upto position +6 to +8, so most likely promoter release is happening after position +8 (Briebe & Sousa, 2001a; Gong et al, 2004; Ikeda & Richardson, 1986; Place et al, 1999). A recent exonuclease III footprinting study also supports the functional correlation of these two events (Guo & Sousa, 2005a). The release of promoter contacts at this stage allows the N-terminal platform to move away from the C-terminal domain

and rearrange itself into a stable elongation phase. Reannealing of the upstream DNA helps in displacement of the 5' end of the RNA into newly forming/formed RNA exit channel (Gong et al, 2004; Jiang et al, 2004; Martin et al, 2005). Those complexes that do not properly displace the RNA into the RNA exit channel become elongation incompetent or dead end complexes, releasing 11-13mer RNA products. Only complexes with proper RNA displacement become bona fide elongation complexes (Gong et al, 2004; Martin et al, 2005).

1.3 Summary:

The main focus of our studies here is the transition from initiation to elongation in T7 RNA polymerase. We have previously reported a model of transition from initiation to elongation (Theis et al, 2004). The studies presented here will be advancement in understanding the process of transition mechanistically and structurally as the polymerase steps through these different translocational phases. In chapter 2, we propose a new model for the abortive cycling, and discussed the different factors affecting the stability of initially transcribing complexes. In chapter 3, we have discussed the different approaches to label the protein (T7 RNA polymerase) site specifically that is important for different FRET measurements (Protein:DNA and Protein:Protein) down the line proposed in our NIH grant.

1.4 References:

- Borukhov S, Lee J, Laptenko O (2005) Bacterial transcription elongation factors: new insights into molecular mechanism of action. *Mol Microbiol* **55**(5): 1315-1324
- Brieba LG, Sousa R (2001a) T7 promoter release mediated by DNA scrunching. *Embo J* **20**(23): 6826-6835
- Brieba LG, Sousa R (2001b) The T7 RNA polymerase intercalating hairpin is important for promoter opening during initiation but not for RNA displacement or transcription bubble stability during elongation. *Biochemistry* **40**(13): 3882-3890.
- Cai H, Luse DS (1987) Variations in template protection by the RNA polymerase II transcription complex during the initiation process. *Mol Cell Biol* **7**(10): 3371-3379.
- Carpousis AJ, Gralla JD (1980) Cycling of ribonucleic acid polymerase to produce oligonucleotides during initiation in vitro at the lac UV5 promoter. *Biochemistry* **19**(14): 3245-3253
- Carpousis AJ, Gralla JD (1985) Interaction of RNA polymerase with lacUV5 promoter DNA during mRNA initiation and elongation. Footprinting, methylation, and rifampicin-sensitivity changes accompanying transcription initiation. *J Mol Biol* **183**(2): 165-177
- Cermakian N, Ikeda T, Cedergren R, Gray M (1996) Sequences homologous to yeast mitochondrial and bacteriophage T3 and T7 RNA polymerases are widespread throughout the eukaryotic lineage. *Nucleic Acids Res* **24**(4): 648-654
- Cheetham GM, Jeruzalmi D, Steitz TA (1999) Structural basis for initiation of transcription from an RNA polymerase- promoter complex. *Nature* **399**(6731): 80-83
- Cheetham GM, Steitz TA (1999) Structure of a transcribing T7 RNA polymerase initiation complex. *Science* **286**(5448): 2305-2309
- Dunn JJ, Studier FW (1983) Complete nucleotide sequence of bacteriophage T7 DNA and the locations of T7 genetic elements. *J Mol Biol* **166**(4): 477-535
- Ebright RH (2000) RNA polymerase: structural similarities between bacterial RNA polymerase and eukaryotic RNA polymerase II. *J Mol Biol* **304**(5): 687-698.
- Esposito EA, Martin CT (2004) Crosslinking of promoter DNA to T7 RNA polymerase does not prevent formation of a stable elongation complex. *J Biol Chem* **279**(43): 44270-44276
- Gong P, Esposito EA, Martin CT (2004) Initial bubble collapse plays a key role in the transition to elongation in T7 RNA polymerase. *J Biol Chem* **279**(43): 44277-44285

- Gopal V, Brieba LG, Guajardo R, McAllister WT, Sousa R (1999) Characterization of Structural Features Important for T7 RNAP Elongation Complex Stability Reveals Competing Complex Conformations and a Role for the Non-template Strand in RNA Displacement. *J Mol Biol* **290**(2): 411-431
- Guillerez J, Lopez PJ, Proux F, Launay H, Dreyfus M (2005) A mutation in T7 RNA polymerase that facilitates promoter clearance. *Proc Natl Acad Sci U S A* **102**(17): 5958-5963
- Guo Q, Nayak D, Brieba LG, Sousa R (2005) Major Conformational Changes During T7RNAP Transcription Initiation Coincide with, and are Required for, Promoter Release. *J Mol Biol*
- Guo Q, Sousa R (2005) Multiple roles for the T7 promoter nontemplate strand during transcription initiation and polymerase release. *J Biol Chem* **280**(5): 3474-3482
- Hansen JL, Long AM, Schultz SC (1997) Structure of the RNA-dependent RNA polymerase of poliovirus. *Structure* **5**(8): 1109-1122
- He B, Rong M, Durbin RK, McAllister WT (1997) A mutant T7 RNA polymerase that is defective in RNA binding and blocked in the early stages of transcription. *J Mol Biol* **265**(3): 275-288
- Hsiou Y, Ding J, Das K, Clark AD, Jr., Hughes SH, Arnold E (1996) Structure of unliganded HIV-1 reverse transcriptase at 2.7 Å resolution: implications of conformational changes for polymerization and inhibition mechanisms. *Structure* **4**(7): 853-860
- Huang J, Sousa R (2000) T7 RNA Polymerase Elongation Complex Structure and Movement. *J Mol Biol* **303**(3): 347-358
- Ikeda RA, Richardson CC (1986) Interactions of the RNA polymerase of bacteriophage T7 with its promoter during binding and initiation of transcription. *Proc Natl Acad Sci U S A* **83**(11): 3614-3618
- Imburgio D, Rong M, Ma K, McAllister WT (2000) Studies of promoter recognition and start site selection by T7 RNA polymerase using a comprehensive collection of promoter variants. *Biochemistry* **39**(34): 10419-10430
- Jaehning JA (1993) Mitochondrial transcription: is a pattern emerging? *Mol Microbiol* **8**(1): 1-4
- Jeruzalmi D, Steitz TA (1998) Structure of T7 RNA polymerase complexed to the transcriptional inhibitor T7 lysozyme. *EMBO J* **17**(14): 4101-4113

- Jia Y, Patel SS (1997) Kinetic mechanism of transcription initiation by bacteriophage T7 RNA polymerase. *Biochemistry* **36**(14): 4223-4232
- Jiang M, Ma N, Vassilyev DG, McAllister WT (2004) RNA displacement and resolution of the transcription bubble during transcription by T7 RNA polymerase. *Mol Cell* **15**(5): 777-788
- Jiang M, Rong M, Martin C, McAllister WT (2001) Interrupting the template strand of the T7 promoter facilitates translocation of the DNA during initiation, reducing transcript slippage and the release of abortive products. *J Mol Biol* **310**(3): 509-522.
- Kohlstaedt LA, Wang J, Friedman JM, Rice PA, Steitz TA (1992) Crystal structure at 3.5 Å resolution of HIV-1 reverse transcriptase complexed with an inhibitor. *Science* **256**(5065): 1783-1790
- Ling ML, Risman SS, Klement JF, McGraw N, McAllister WT (1989) Abortive initiation by bacteriophage T3 and T7 RNA polymerases under conditions of limiting substrate [published erratum appears in *Nucleic Acids Res* 1989 Jun 12;17(11):4430]. *Nucleic Acids Res* **17**(4): 1605-1618
- Liu C, Martin CT (2001) Fluorescence characterization of the transcription bubble in elongation complexes of T7 RNA polymerase. *J Mol Biol* **308**(3): 465-475.
- Liu C, Martin CT (2002) Promoter clearance by T7 RNA polymerase. Initial bubble collapse and transcript dissociation monitored by base analog fluorescence. *J Biol Chem* **277**(4): 2725-2731
- Lopez PJ, Guillerez J, Sousa R, Dreyfus M (1997) The low processivity of T7 RNA polymerase over the initially transcribed sequence can limit productive initiation in vivo. *J Mol Biol* **269**(1): 41-51
- Ma K, Temiakov D, Anikin M, McAllister WT (2005) Probing conformational changes in T7 RNA polymerase during initiation and termination by using engineered disulfide linkages. *Proc Natl Acad Sci U S A* **102**(49): 17612-17617
- Martin CT, Esposito EA, Theis K, Gong P (2005) Structure and Function in Promoter Escape by T7 RNA Polymerase. *Prog Nucl Acid Res Mol Biol* **80**: 323-347
- Martin CT, Muller DK, Coleman JE (1988) Processivity in early stages of transcription by T7 RNA polymerase. *Biochemistry* **27**(11): 3966-3974
- McAllister WT (1993) Structure and function of the bacteriophage T7 RNA polymerase (or, the virtues of simplicity). *Cell Mol Biol Res* **39**(4): 385-391
- McAllister WT (1997) Transcription by T7 RNA polymerase. *Nucleic Acids Mol Biol* **11**: 15-25

- Milligan JF, Groebe DR, Witherell GW, Uhlenbeck OC (1987) Oligoribonucleotide synthesis using T7 RNA polymerase and synthetic DNA templates. *Nucleic Acids Res* **15**(21): 8783-8798
- Moroney SE, Piccirilli JA (1991) Abortive products as initiating nucleotides during transcription by T7 RNA polymerase. *Biochemistry* **30**(42): 10343-10349
- Mukherjee S, Brieba LG, Sousa R (2003) Discontinuous movement and conformational change during pausing and termination by T7 RNA polymerase. *Embo J* **22**(24): 6483-6493
- Muller DK, Martin CT, Coleman JE (1988) Processivity of proteolytically modified forms of T7 RNA polymerase. *Biochemistry* **27**(15): 5763-5771
- Place C, Oddos J, Buc H, McAllister WT, Buckle M (1999) Studies of contacts between T7 RNA polymerase and its promoter reveal features in common with multisubunit RNA polymerases. *Biochemistry* **38**(16): 4948-4957
- Schroeder LA, deHaseth PL (2005) Mechanistic differences in promoter DNA melting by *Thermus aquaticus* and *Escherichia coli* RNA polymerases. *J Biol Chem* **280**(17): 17422-17429
- Sousa R, Chung YJ, Rose JP, Wang BC (1993) Crystal structure of bacteriophage T7 RNA polymerase at 3.3 Å resolution. *Nature* **364**(6438): 593-599
- Sousa R, Rose J, Wang B (1994) The thumb's knuckle. Flexibility in the thumb subdomain of T7 RNA polymerase is revealed by the structure of a chimeric T7/T3 RNA polymerase. *J Mol Biol* **244**(1): 6-12
- Stano NM, Patel SS (2002) The intercalating beta-hairpin of T7 RNA polymerase plays a role in promoter DNA melting and in stabilizing the melted DNA for efficient RNA synthesis. *J Mol Biol* **315**(5): 1009-1025
- Steitz TA (1999) DNA polymerases: structural diversity and common mechanisms. *J Biol Chem* **274**(25): 17395-17398
- Tahirov TH, Temiakov D, Anikin M, Patlan V, McAllister WT, Vassilyev DG, Yokoyama S (2002) Structure of a T7 RNA polymerase elongation complex at 2.9 Å resolution. *Nature* **420**(6911): 43-50
- Temiakov D, Patlan V, Anikin M, McAllister WT, Yokoyama S, Vassilyev DG (2004) Structural basis for substrate selection by t7 RNA polymerase. *Cell* **116**(3): 381-391
- Újvári A, Martin CT (1996) Thermodynamic and kinetic measurements of promoter binding by T7 RNA polymerase. *Biochemistry* **35**(46): 14574-14582

Yin YW, Steitz TA (2002) Structural basis for the transition from initiation to elongation transcription in T7 RNA polymerase. *Science* **298**(5597): 1387-1395

Yin YW, Steitz TA (2004) The structural mechanism of translocation and helicase activity in T7 RNA polymerase. *Cell* **116**(3): 393-404

CHAPTER 2

Abortive Cycling in T7 RNA Polymerase

2.1 Introduction:

Like other DNA dependent RNA polymerases, T7 RNA polymerase binds to promoter DNA and carries out *de novo* transcription. T7 RNA polymerase carries out each step of transcription cycle in a fashion similar to that of the multisubunit RNA polymerases (McAllister, 1997). Moreover, T7 RNA polymerase is a single subunit enzyme, capable of carrying out the transcription cycle without the help of any auxiliary co-factors, which makes it an attractive model to study fundamental aspects of transcription. Many studies including fluorescence approaches and footprinting (Gunderson and Burgess, biochemistry, 1987, Ikeda et al, PNAS, 1986, Liu and Martin, JBC, 2002), have shown that T7 RNA polymerase recognizes and binds the promoter DNA sequence, melts open the DNA to form an initiation bubble positioned at +1 position (the start site) in the active site and then maintains promoter contacts as transcription begins, forming an unstable initiation complex (IC), which synthesizes and releases 2-8 mer short abortive transcripts (Carpousis & Gralla, 1980; Lescure et al, 1981; Martin et al, 1988; Milligan et al, 1987). T7 RNA polymerase (RNAP) enters into a stable processive elongation phase after synthesizing 9-10 bases of RNA and loses the promoter contacts at the same time. The elongation complex extends RNA chain in a sequence independent manner (Cai & Luse, 1987; Carpousis & Gralla, 1985; Ikeda & Richardson, 1986). These characteristics of T7 RNA polymerase are similar to those of the multisubunit RNA polymerases (Borukhov & Nudler, 2003; Murakami & Darst, 2003).

The single subunit structure of T7 RNA polymerase makes it an ideal model enzyme in which to study the complex process of transcription. This simple and unique enzyme carries out all of the processes of transcription such as initiation, abortive cycling, and the transition to a stable elongation complex, and termination. Growth of the RNA: DNA hybrid is supposed to be the driving force for the initial movement of the N-terminal domain (1-266 residues) of the T7 RNA polymerase during the early phases of transcription (Tahirov et al, 2002; Yin & Steitz, 2002). The growing hybrid is also responsible for the disruption of contacts between RNA polymerase and promoter DNA. As soon as the promoter contacts are lost, the topological constraints disappear from the system allowing the polymerase to undergo conformational changes to establish a stable elongation conformation (Theis et al, 2004). To understand the mechanism of abortive cycling and transition to elongation, it is very important to learn the individual contributions of RNA, DNA and enzyme to the stability of intermediate complexes.

The understanding of the newly established relationship between initial bubble collapse and initial RNA displacement has shed some light on a more illustrated model in the late stages of the transition (Gong et al, 2004; Martin et al, 2005). Based on our recent data, we have proposed that the complexes with proper initial RNA displacement can undergo the transition and achieve stable elongation conformation. Complexes that are not able to properly displace the 5' end of the nascent RNA chain will result in a few more nucleotide additions before dissociation of 11- 13 mer dead end products. The release of 2-8 mer abortive products during early stages of transcription arises from the inherent instability of the initially transcribing complexes (Mentesana et al, 2000; Tahirov et al, 2002). According to recent evidence, the retention of promoter contacts

might compete with the forward movement of polymerase along the template DNA strand toward elongation phase (Guo & Sousa, 2005b), as proposed in *E.Coli* RNA polymerase (Carpousis & Gralla, 1980; Straney & Crothers, 1987a; Straney & Crothers, 1987b). The retention of promoter contacts might be playing a dual role here. On the one hand, retention of these contacts makes the initially transcribing complex unstable, which leads to the release of abortive products, while on the other hand it might also trigger promoter release, ultimately forming a processive stable elongation complex (Briebe & Sousa, 2001a). The RNA polymerase finally adopts an energetically favorable conformation as in the promoter bound complex or in an initiation complex with a 3 mer RNA transcript (Cheetham et al, 1999; Cheetham & Steitz, 1999; Sousa et al, 1993). The intermediate RNA polymerase conformations prior to the formation of elongation complex are expected to be less favorable. Therefore, a potential factor contributing towards abortive cycling could be the competition between the lengthening RNA:DNA hybrid triggering the structural change and the folding back of unstable intermediate complexes to the initiation conformation (Tahirov et al, 2002). This entire model could be a means to understand the different pathways that can lead to the release/production of abortive transcripts. Understanding the mechanism of release of abortive products may suggest ways to control the level of abortive products profile.

Transcription bubble collapse is the other important factor that contributes to the abortive cycling. However, there is some evidence that transcription from partially single stranded DNA, DNA lacking the non-template strand in the transcribing region, which is unable to undergo collapse, shows an abortive transcription profile similar to that of transcription from duplex DNA constructs (Martin et al, 1988). Whereas the evidence

(i.e. less abortive products at +6 position in a similar partially single stranded DNA constructs) suggests that the transcription bubble collapse could be a factor for instability of abortive complexes (Diaz et al, 1996). Recent data from our lab have revealed a potential role of transcription bubble collapse in the initiation phase. More specifically we have proposed a model in which collapse from the downstream end of the bubble is a major factor that contributes to the instability of the intermediate transcription complexes (Gong & Martin, 2006). In this case, collapse from the downstream end of the transcription bubble leads to the displacement of the 3' end of the RNA before the transition position +8. This collapse effectively halts transcription process because the growing end of the RNA chain is out of enzyme's active site and ultimately facilitates the release of abortive products. This case is different from the collapse of transcription bubble from *upstream* end induced by promoter release on translocation beyond +8 position, which is important for the initial displacement of the 5' end of the growing RNA chain.

In previous work from our lab by Gong et. al., 2006, we have shown that there is an enhancement in the stability of the initially transcribing complexes throughout the transition process to elongation by weakening the promoter contacts. This enhancement directly suggests that promoter contacts play a critical role in the instability of the intermediate complexes. Here, we continued the further characterization of the abortive cycling in the runoff transcription assays. From all our data and previous work from other groups, we came up with the following model for abortive cycling in the runoff transcripts.

2.2 An integrated model for abortive cycling:

As with all RNA polymerases, T7 RNA polymerase engages in abortive cycling before it achieves processive elongation (Carpousis & Gralla, 1980; Martin et al, 1988; Milligan et al, 1987). Abortive cycling is characterized by the rapid dissociation of short RNA transcripts followed by a second round of RNA synthesis (reinitiation). However, the mechanism of the instability of abortive cycling in RNA polymerase has not been well understood. Studies in the past few years and emerging data from our lab and others have inspired us to come up with an integrated mechanistic model for abortive cycling in T7 RNA polymerase (Figure 2.1):

1). When the RNA chain is about 2-3 bases long (close to state 3 in Figure 2.1), the protein still adopts the initial and stable conformation (Cheetham & Steitz, 1999; Sousa et al, 1993). The enzyme maintains an open bubble. The instability of the complex comes solely from the instability of the short DNA-RNA hybrid.

2). As the RNA chain extends to about 4-8 bases, the hybrid gets longer and presumably becomes more stable by itself. Other elements within the initially transcribing complex now come into play:

a) As suggested by structural data (Cheetham & Steitz, 1999; Tahirov et al, 2002; Yin & Steitz, 2002), steric clash between the growing hybrid and the N-terminal domain occurs at or after the synthesis of a 3-base RNA, resulting in the N-terminal domain moving away from the active site. Different structural models have been proposed to describe this movement (Tahirov et al, 2002; Theis et al, 2004), but in any case the initial stable conformation of the protein is disrupted to some extent and relatively unstable intermediate conformations are produced. That steric clash between

N-terminal domain and growing hybrid presumably contributes significantly to the instability of the complex.

b) The retention of promoter contacts at this stage plays dual roles and is closely related to the fate of the released RNA. First, retention of promoter contacts does not allow the final establishment of the elongation mode protein-nucleic acid interactions and maintains the complex in a strained state. Moreover, it provides a simple path for the strained protein to "relax back" to the initial stable conformation (a pathway similar to state 4 to state 3 transition shown in Figure 2.1).

c) Practically, a "relaxing back" requires a shortening of the hybrid from the RNA 3' end which can be facilitated by DNA rewinding from the downstream end (Gong & Martin, 2006). This backward movement, as compared to the forward pathway from state 3 to state 4 in Fig. 2.1, would result in relaxation of the conformational strain in the complex and shortening of the hybrid. The latter would lower the barrier to release of the RNA transcript as illustrated in Figure 2.1 (the pathway from state 4 to state 3 through intermediate state 8).

3). In contrast to relaxing the strain by allowing the protein to relax back towards its initial configuration while releasing the RNA from its 3' end; the complex can achieve a new stable state by releasing promoter contacts and forming the elongation mode protein-nucleic acid interactions. At some point, these two pathways exist in a competitive manner with RNA release favored at translocational positions +8 or +9 and promoter release favored thereafter, as suggested by various studies (Diaz et al, 1996; Gong & Martin, 2006; Guo & Sousa, 2005b; Liu & Martin, 2002; Tang et al, 2005). Conceivably, a complex stepped beyond position +8 that has undergone rotation final of the N-terminal

domain (species 4 to 5 in figure 2.1) can no longer relax back to or adopt an initial conformation (represented by state 2 in Figure 2.1).

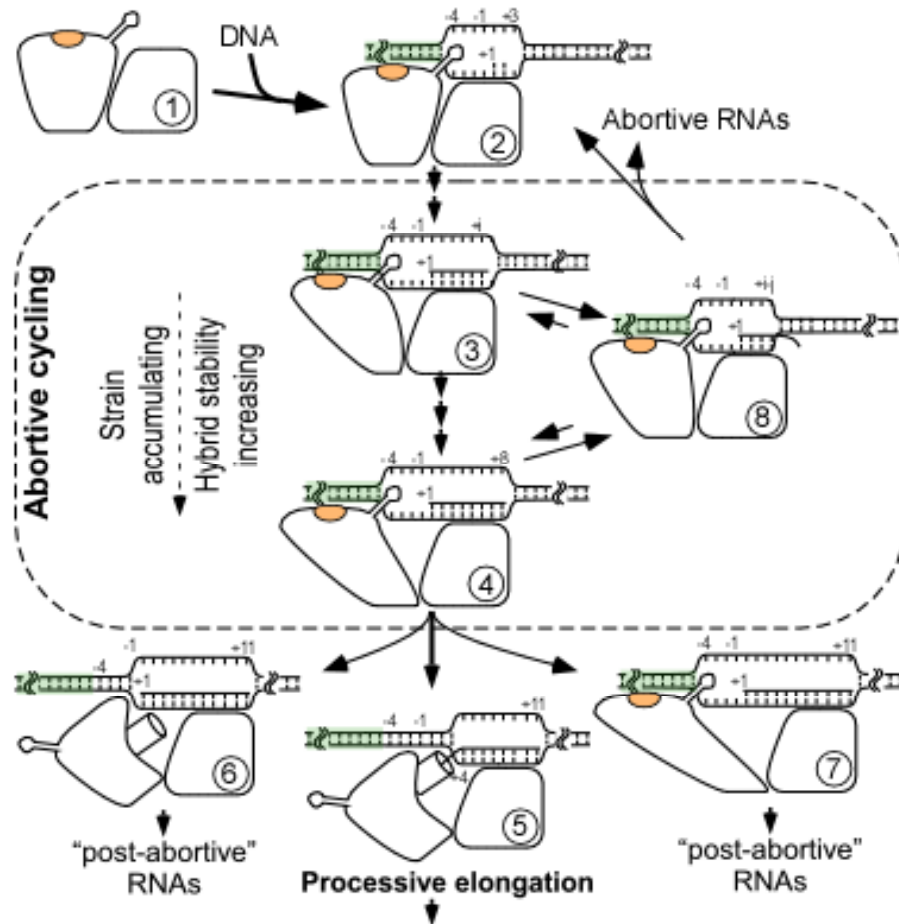


Figure 2.1: A model for abortive cycling

The productive path follows states from 1 through 5. States 3 to 4 represent translational position +3 through about +8 or +10, with both strain and stability building in the system. In state 5, promoter contacts have been released, the N-terminal domain has rotated, the upstream edge of the bubble has collapsed, and the 5' end of the RNA has been properly displaced into the exit channel. States 6 and 7 represent states containing “extended hybrids,” with or without promoter release and rotation of the N-terminal domain. State 8 (potentially transient) represents a proposed intermediate for abortive release in which the downstream edge of the bubble has collapsed.

4). In summary, we define abortive cycling in T7 RNA polymerase by two major properties: First, the retention of promoter contacts; second, a high tendency of polymerase to relax back to the initial and stable conformation, releasing the nascent transcript.

2.3 Results:

2.3.1 Instability of the Abortive Complexes due to the Transcription Bubble Collapse from the Downstream End

It has been proposed that the reannealing of the DNA bubble makes initially transcribing complexes unstable (Diaz et al, 1996; Guo & Sousa, 2005a; Montesana et al, 2000). Our previous data on abortive complexes have shown that transcription bubble collapse from the upstream end of the bubble does not contribute to the instability of the partially single stranded stalled complexes (Gong et al, 2004; Gong & Martin, 2006). Rather, it is reannealing from the downstream end of the bubble that more likely contributes to the instability of the complex. However, the data presented here (fig. 2.2) reveal that introduction of mismatches from positions +2 to +4 leads to an increase in the amount of 4-6mer abortive product relative to full length runoff product. It is too early to say that the bubble collapse from the upstream end contributes to the instability of the abortive complexes. On the other hand, it could be just the inherent instability of the short 2 to 3 mer RNA transcripts. However, the reannealing of the DNA from the upstream end at the appropriate time is very critical for the proper displacement of the 5' end of the nascent RNA chain into the initially forming/formed RNA exit channel.

In previous work by Gong & Martin, 2006, it was shown that prevention of bubble collapse at the downstream end of the transcription bubble enhances the stability of initially transcribing complexes halted by nucleotide omission. Based on these results, we hypothesized that it might be possible to minimize abortive products by introducing modifications into DNA designed to increase the stability of initially transcribing complexes by reducing the energetics of downstream bubble collapse (e.g. mismatches, nicks, gaps, spacers, and linkers). To test our hypothesis we selected the *lac* sequence

(see fig. 2.2 A), which is known to abort excessively. Then, we modified the non-template strands of the duplex *lac* sequence to introduce a mismatch of three bases at different positions i.e. +2 to +4, +4 to +6, and +6 to +8 positions (see fig. 2.2B). First, all sets of DNA constructs have been characterized in a transcription assays (see Materials and Methods) using both wild type RNA polymerase and a mutant polymerase (P266L) known to produce fewer abortive transcripts. We can directly test the above predictions by comparing the accumulation of abortive RNA products.

The data presented in Figure 2.2C demonstrate that constructs containing mismatched DNA from position +4 to +6 yield fewer abortives in both wild type and P266L mutant enzyme, as predicted by the model. The contributing factors (as discussed in model) in this case are; i) as the nascent RNA chain extends to about 4-8 bases, the hybrid gets longer and presumably becomes more stable by itself, ii) another factor contributing to this stability is the mismatch at +6 to +8 position in non-template strand, avoiding the bubble collapse from downstream and making more favorable condition for complex to enter into stable elongation confirmation. However, +2 to +4 mismatched DNA constructs produce nearly the same amount of abortive, transcripts in wild type and somewhat more abortive in the P266L mutant enzyme than do constructs having mismatches from position +4 to +6 and +6 to +8 and than the control without any mismatch. This result was not expected based on our model. It seems that the downstream bubble collapse does not have a pronounced effect in the initially transcribing complexes having mismatches at position +2 to +4. In these complexes, the RNA chain is about 2-3 bases long in the mismatch region +2 to +4 and the DNA: RNA hybrid is very short, which makes the complex unstable. Incorporation of another

an *earlier* promoter release and transition to a stable elongation complex (Guillerez et al, 2005). In contrast, the E148A mutation results in a substantial increase in the relative amount of shorter (5-6mer) abortive products (He et al, 1997). This mutation could destabilize early translational states by 1) destabilizing the complex to promoter retention, leading to early promoter release, or 2) limiting the N-terminal platform translocation. In the first case, release at this early stage would likely lead to invasive collapse of the bubble onto a relatively unstable hybrid. In the second case, promoter would remain bound, but the RNA would fail to extend.

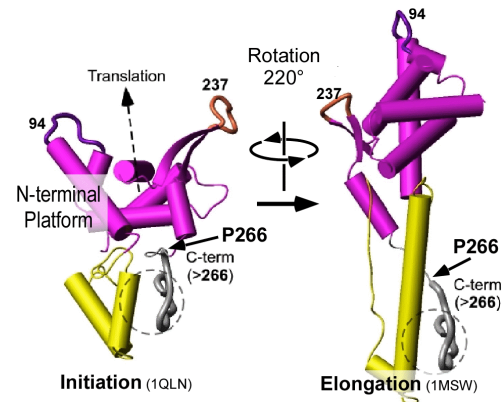


Fig 2.3 P266L lies in a region that undergoes substantial structural change.

2.3.2 Effect of NTP concentration on the abortive profile of mismatched DNA constructs

It has been reported earlier that class II termination is more efficient at high NTP concentrations, and it was suggested that this was due to a requirement for high NTP concentrations to maintain a termination-prone conformation of the enzyme (Song & Kang, 2001). It was suggested that low CTP concentrations reduce termination because it prolongs the *n* pause, a pause site before termination, thus extending the time during which the polymerase may release the upstream interactions. While high CTP concentrations drive the polymerase rapidly to *n*+ 1 while it is still engaged with the class II element and where increased strain can then drive a conformational change that leads to termination. Several groups have proposed that termination is analogous to the reversal

of transcription initiation process (Briebe et al, 2001; Cheetham et al, 1999; Cheetham & Steitz, 1999; Mukherjee et al, 2002; Temiakov et al, 2000). Therefore, a question arises: do we see an effect of increased NTP concentrations on abortive profiles? To answer this question, we use the same DNA constructs as in figure 2.2, and the transcription reaction was performed with twice the concentration (1600 μ M) of NTPs used in the previous reaction (fig.2.2). The preincubation time (1 minute) of DNA and enzyme, the ratio of DNA:Enzyme (1:1), and the transcription reaction time (5 min) were the same as that of the reaction explained in figure 2.2. As shown in the results in figure 2.4, we did not see any effect of increased NTP concentrations during transcription initiation. All the constructs behave in a similar fashion as they do in the previous experiment (compare with figure 2.2).

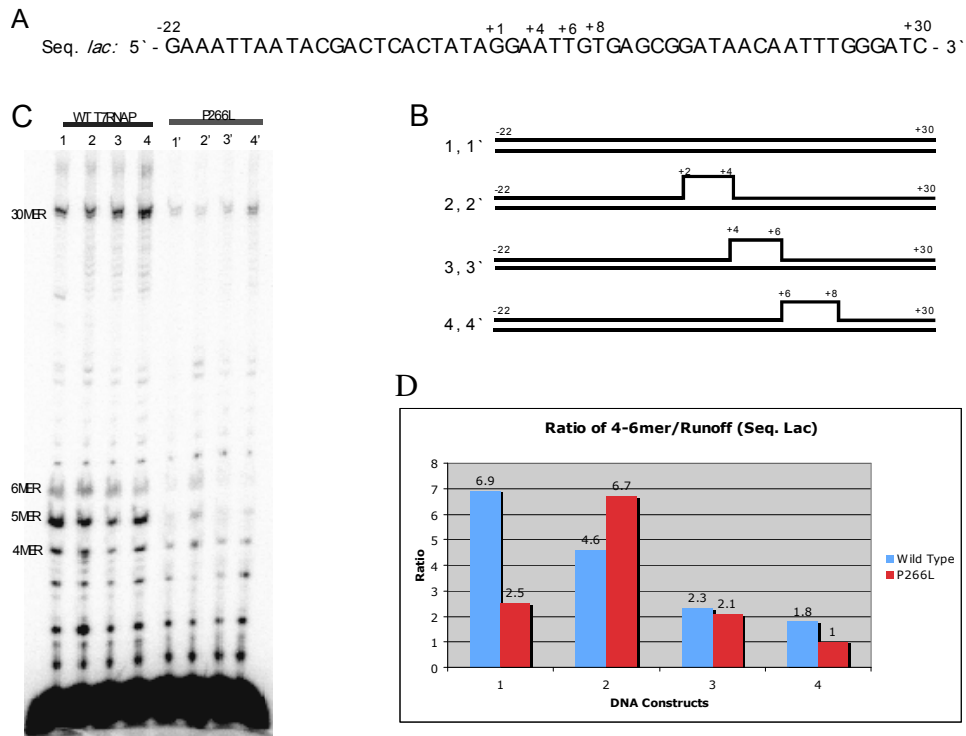


Figure 2.4: Effect of NTP concentrations on abortive profiles

A) *lac* sequence (non template), B) Constructs design, C) Abortive profile of *lac* modified sequence, D) Ratio of (+4 to +6 mer) to run off transcripts.

2.3.3 Characterization of abortive complexes in runoff transcription reaction:

Abortive cycling in mismatched complexes – As shown in figure 2.2 and 2.4, abortive profile in DNA complexes with mismatches (MM) at +4 to +6 and +6 to +8 are behaving as expected, (i.e. the profiles show lower abortive products due to the reduction in collapse from the downstream edge of the transcription bubble). However, the mismatch +2 to +4 complexes do not show a similar reduction. That is likely due to a different primary mechanism for release of very short RNA's. Their inherent instability is likely more dominant than collapse-mediated instability.

Abortive cycling in mismatched and nicked complexes – The data presented in figure 2.5 shows the abortive profile of sequences that were tested for high abortive products with mismatches from +4 to +6 and nicks between +6 & +7, and +8 & +9. One might expect nicks to behave similar to mismatch complexes (Rong et al, 1998). Nevertheless, the results presented here are contradictory to the reported behavior of nicked complexes. The nick in between +6 & +7 should be essentially similar to mismatch at +4 to +6 complexes, and nick in between +8 & +9 should be similar to mismatch at +6 to +8 complexes. As the mismatches at +4 to +6 and +6 to +8 are shown to decrease the abortive products, therefore the nicked complexes are also expected to do so. However as we can see in lane 4 in figure 2.5, abortive products are even much higher than the other complexes, showing that nicked constructs behave differently (in terms of abortive cycling) than the mismatched complexes. Therefore, we decided to study the abortive cycling in mismatched and nicked constructs separately and with increased reaction time.

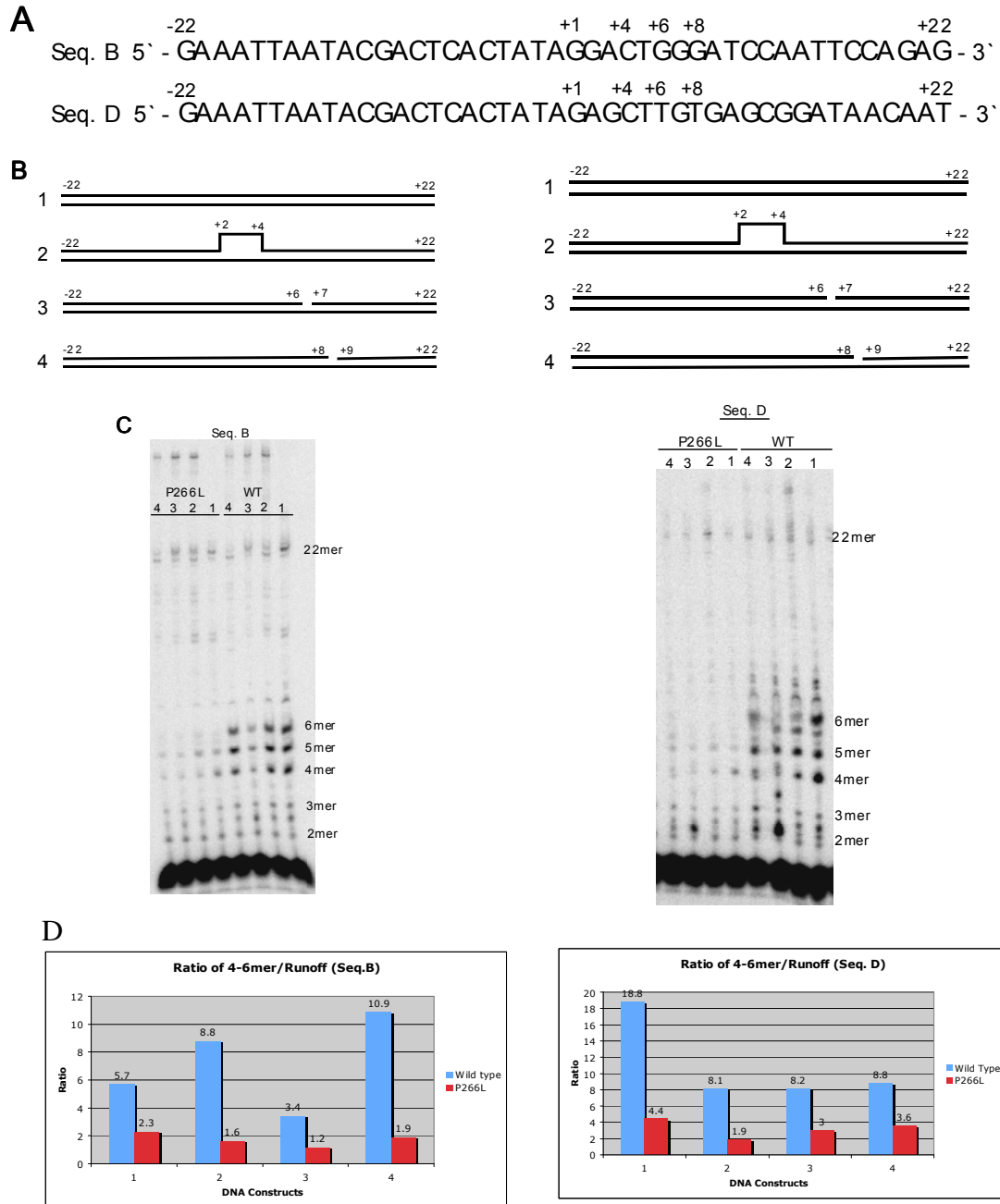


Figure 2.5: Comparison of abortive profiles to see the effect of mismatches and nicks modifications in DNA constructs.

A) Seq. B and Seq. D (non template), B) Constructs design, C) Abortive profile of modified sequences, D) Ratio of (+4 to +6 mer) to runoff transcripts.

Abortive cycling in mismatched constructs with increased reaction time- In some of the previous transcription reactions, the runoff product band was faint, was not visible, or

in other words may be less runoff product was formed. To avoid this problem the reaction time was increased from 5 minute to 15 minute while keeping the other conditions same as that of before. The data presented in figure 2.6 is the abortive product profile of sequences (with mismatches) B, D and *lac* (L) with increased reaction time. As we can observe here, the trend of abortive profile is similar to what we have seen in 5-minute reaction time. The lines labeled as GA are controls with respective wild type DNA constructs of each sequences because they only includes GTP and ATP in the reaction (i.e. B, D and, Lac; should be forming 3mer, 3mer and, 4mer respectively). However, all sequences form higher band that may be due to misincorporation of NTPs or something else. The abortive profile data from DNA constructs having mismatches at position +4 to +6 and +6 to +8 supports our integrated model of abortive cycling. DNA constructs containing mismatch at position +2 to +4 need to be further characterized to understand their unexpected behavior because they do not fit our model of abortive cycling.

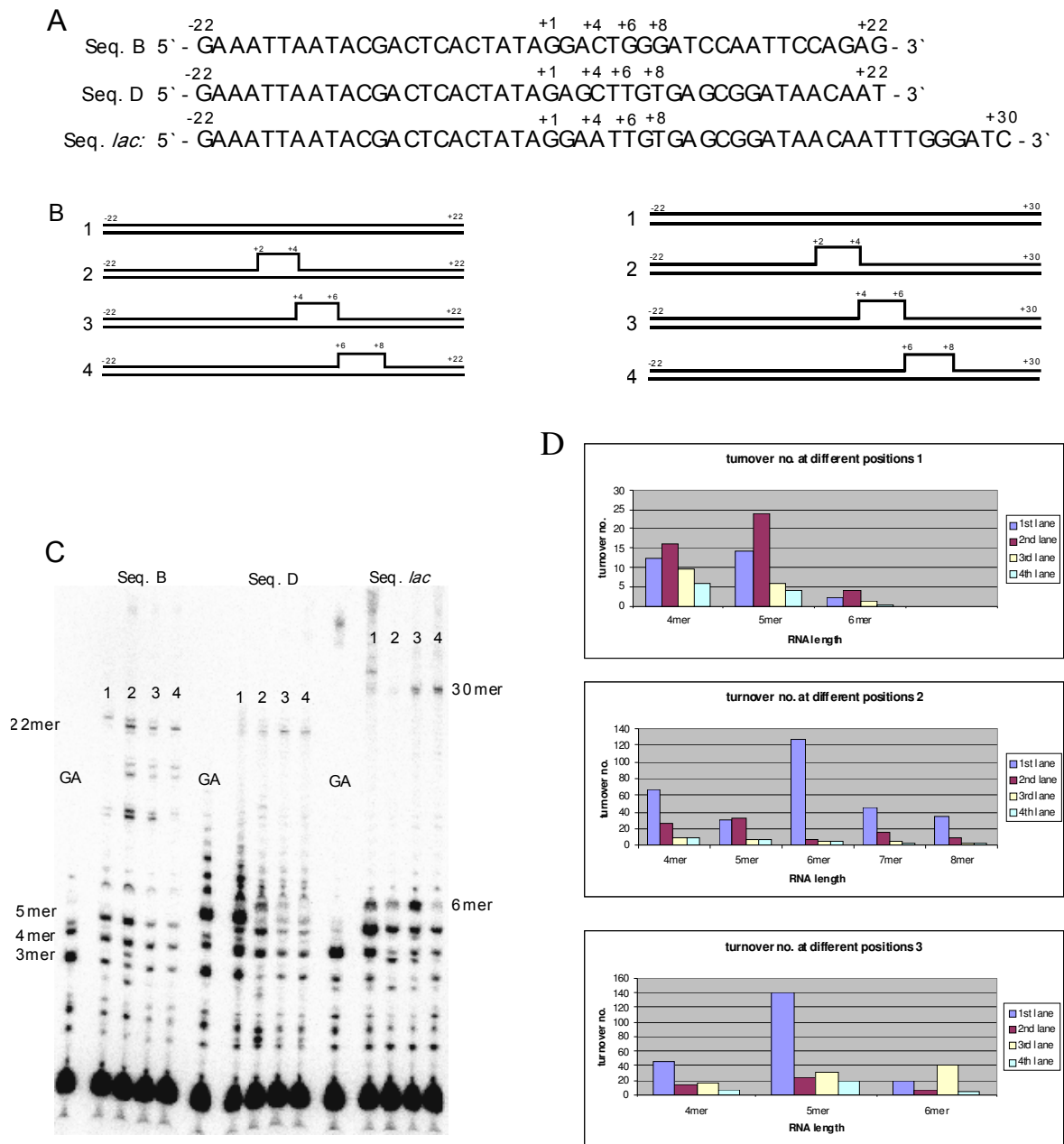


Figure 2.6: Abortive profile of mismatched DNA constructs

A) Seq. B, Seq. D, and Seq. *lac* (non template), B) Constructs design, C) Abortive profile of modified sequences, D) Turnover number at different positions.

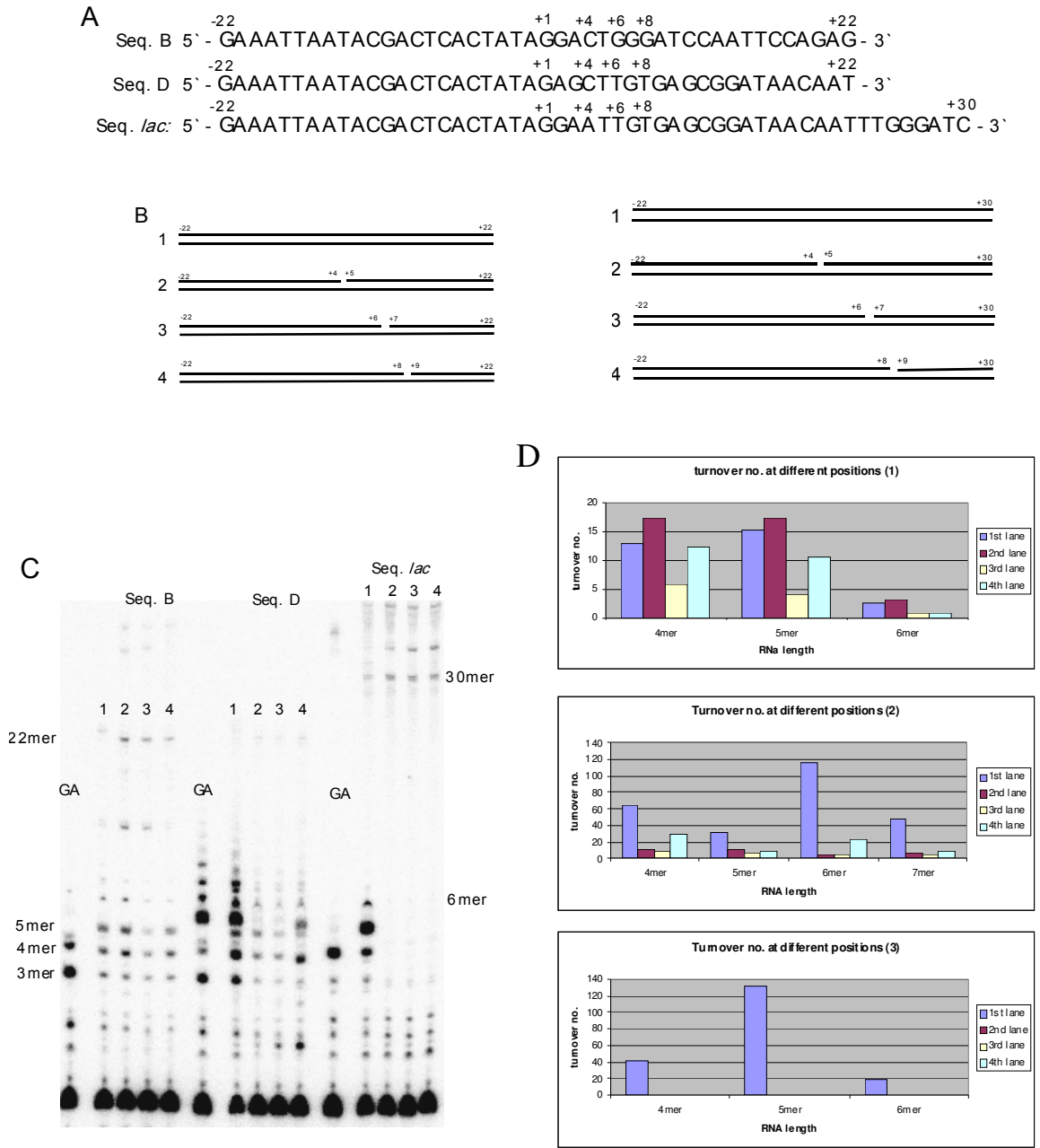


Figure 2.7: Abortive profile of nicked DNA constructs

A) Seq. B, Seq. D, and Seq. *lac* (non template), B) Constructs design, C) Abortive profile of modified sequences, D) Turnover number at different positions.

Abortive cycling in nicked constructs with increased reaction time- The data for abortive cycling of nicked constructs from sequences B, D and, *Lac* (L) is presented in figure 2.7. It is very clear from these data that the abortive cycling behavior of nicked constructs is different from the mismatched constructs. The DNA constructs containing nicks from *lac* sequence show more pronounced effect in reducing abortive products than the other two sequences (Seq. B and Seq. D). All nicked constructs used in this study, strongly support our model. In Seq. B, the first three constructs (i.e. wild type constructs), containing nicks at position +4 - +5, and +6 - +7 show considerable amounts of 11-13mer dead end products. These dead end products are not present in the other two sequences i.e. Seq. D, and Seq. *lac*. However, other than Seq. D, the remaining two sequences produce a higher band than the runoff transcript, which makes the quantification of the abortive products ratios difficult.

2.4 Materials and Method

2.4.1 Protein expression and purification

His-tagged wild type and mutant T7 RNA polymerase were over expressed in *E. coli* strain BL21 and purified using Qiagen Ni-NTA column material. The fractions collected from Ni-NTA column were further purified by Toyopearl ion-exchange columns such as CM - 650 M and DEAE - 650 M columns from Tosoh Bioscience. Protein purity was determined by SDS-PAGE gel analysis. The purified protein was concentrated and dialyzed against 100 mM NaCl, storage buffer pH 7.8 (1.6 mM KH₂PO₄, 18.2 mM K₂HPO₄, 50% glycerol and 1 mM Na₂EDTA) and stored at -20°C. Concentration was calculated from the measured absorbance at 280 nm using the molar extinction coefficient of $1.4 \times 10^5 \text{M}^{-1} \text{cm}^{-1}$. Activity was determined by a “transcription assay” described below.

2.4.2 Oligonucleotide synthesis and purification

DNA oligos were synthesized trityl-off using an Applied Biosystems Expedite 8909 DNA synthesizer, PAGE purified, excised from the gel, and eluted using an Elu-Trap® device. (Schleicher and Schuell Inc., Keene, NH) Concentrations of single strand DNAs were determined by U-2000 UV-Vis Spectrometer (Hitachi). Single strand DNAs were stored at -20°C.

2.4.3 Double stranded or partially single stranded DNA construction

Non-template DNA and the relevant template DNA were combined in equal molar concentrations, heated to 75°C, and then cooled slowly to room temperature for annealing. Annealed DNA constructs were stored at -20°C.

2.4.4 Transcription assays

Experiments were carried out in a total volume of 16 μ L at 37°C for 5 minutes before being quenched with an equal volume of formamide stop solution (95% formamide, 40 mM EDTA, 0.02% bromophenol blue). Equal molar concentrations of DNA construct and enzyme were used at final concentrations of 0.125 μ M in a reaction buffer containing 30 mM HEPES at pH 7.8, 15 mM magnesium acetate, 25 mM potassium glutamate, 0.25 mM EDTA, 0.05% Tween 20. Reactions were initiated by addition of NTP's to a final concentration of 400 μ M each and labeled with α 32P-GTP.

2.5 References:

Borukhov S, Lee J, Laptenko O (2005) Bacterial transcription elongation factors: new insights into molecular mechanism of action. *Mol Microbiol* **55**(5): 1315-1324

Brieba LG, Gopal V, Sousa R (2001) Scanning mutagenesis reveals roles for helix n of the bacteriophage T7 RNA polymerase thumb subdomain in transcription complex stability, pausing, and termination. *J Biol Chem* **276**(13): 10306-10313.

Brieba LG, Sousa R (2001a) T7 promoter release mediated by DNA scrunching. *Embo J* **20**(23): 6826-6835

Brieba LG, Sousa R (2001b) The T7 RNA polymerase intercalating hairpin is important for promoter opening during initiation but not for RNA displacement or transcription bubble stability during elongation. *Biochemistry* **40**(13): 3882-3890.

Cai H, Luse DS (1987) Variations in template protection by the RNA polymerase II transcription complex during the initiation process. *Mol Cell Biol* **7**(10): 3371-3379.

Carpousis AJ, Gralla JD (1980) Cycling of ribonucleic acid polymerase to produce oligonucleotides during initiation in vitro at the lac UV5 promoter. *Biochemistry* **19**(14): 3245-3253

Carpousis AJ, Gralla JD (1985) Interaction of RNA polymerase with lacUV5 promoter DNA during mRNA initiation and elongation. Footprinting, methylation, and rifampicin-sensitivity changes accompanying transcription initiation. *J Mol Biol* **183**(2): 165-177

Cermakian N, Ikeda T, Cedergren R, Gray M (1996) Sequences homologous to yeast mitochondrial and bacteriophage T3 and T7 RNA polymerases are widespread throughout the eukaryotic lineage. *Nucleic Acids Res* **24**(4): 648-654

Cheetham GM, Jeruzalmi D, Steitz TA (1999) Structural basis for initiation of transcription from an RNA polymerase- promoter complex. *Nature* **399**(6731): 80-83

Cheetham GM, Steitz TA (1999) Structure of a transcribing T7 RNA polymerase initiation complex. *Science* **286**(5448): 2305-2309

Diaz GA, Rong M, McAllister WT, Durbin RK (1996) The stability of abortively cycling T7 RNA polymerase complexes depends upon template conformation. *Biochemistry* **35**(33): 10837-10843

Dunn JJ, Studier FW (1983) Complete nucleotide sequence of bacteriophage T7 DNA and the locations of T7 genetic elements. *J Mol Biol* **166**(4): 477-535

Ebright RH (2000) RNA polymerase: structural similarities between bacterial RNA polymerase and eukaryotic RNA polymerase II. *J Mol Biol* **304**(5): 687-698.

Esposito EA, Martin CT (2004) Crosslinking of promoter DNA to T7 RNA polymerase does not prevent formation of a stable elongation complex. *J Biol Chem* **279**(43): 44270-44276

Gong P, Esposito EA, Martin CT (2004) Initial bubble collapse plays a key role in the transition to elongation in T7 RNA polymerase. *J Biol Chem* **279**(43): 44277-44285

Gong P, Martin CT (2006) Mechanism of instability in abortive cycling by T7 RNA polymerase. *J Biol Chem* **281**(33): 23533-23544

Gopal V, Briebe LG, Guajardo R, McAllister WT, Sousa R (1999) Characterization of Structural Features Important for T7 RNAP Elongation Complex Stability Reveals Competing Complex Conformations and a Role for the Non-template Strand in RNA Displacement. *J Mol Biol* **290**(2): 411-431

Guillerez J, Lopez PJ, Proux F, Launay H, Dreyfus M (2005) A mutation in T7 RNA polymerase that facilitates promoter clearance. *Proc Natl Acad Sci U S A* **102**(17): 5958-5963

Guo Q, Nayak D, Briebe LG, Sousa R (2005) Major Conformational Changes During T7RNAP Transcription Initiation Coincide with, and are Required for, Promoter Release. *J Mol Biol*

Guo Q, Sousa R (2005a) Multiple roles for the T7 promoter nontemplate strand during transcription initiation and polymerase release. *J Biol Chem* **280**(5): 3474-3482

Guo Q, Sousa R (2005b) Weakening of the T7 promoter:Polymerase interaction facilitates promoter release. *J Biol Chem* **280**(15): 14956-14961

Hansen JL, Long AM, Schultz SC (1997) Structure of the RNA-dependent RNA polymerase of poliovirus. *Structure* **5**(8): 1109-1122

He B, Rong M, Durbin RK, McAllister WT (1997) A mutant T7 RNA polymerase that is defective in RNA binding and blocked in the early stages of transcription. *J Mol Biol* **265**(3): 275-288

Hsiou Y, Ding J, Das K, Clark AD, Jr., Hughes SH, Arnold E (1996) Structure of unliganded HIV-1 reverse transcriptase at 2.7 Å resolution: implications of conformational changes for polymerization and inhibition mechanisms. *Structure* **4**(7): 853-860

Huang J, Sousa R (2000) T7 RNA Polymerase Elongation Complex Structure and Movement. *J Mol Biol* **303**(3): 347-358

Ikeda RA, Richardson CC (1986) Interactions of the RNA polymerase of bacteriophage T7 with its promoter during binding and initiation of transcription. *Proc Natl Acad Sci U S A* **83**(11): 3614-3618

Imburgio D, Rong M, Ma K, McAllister WT (2000) Studies of promoter recognition and start site selection by T7 RNA polymerase using a comprehensive collection of promoter variants. *Biochemistry* **39**(34): 10419-10430

Jaehning JA (1993) Mitochondrial transcription: is a pattern emerging? *Mol Microbiol* **8**(1): 1-4

Jeruzalmi D, Steitz TA (1998) Structure of T7 RNA polymerase complexed to the transcriptional inhibitor T7 lysozyme. *EMBO J* **17**(14): 4101-4113

Jia Y, Patel SS (1997) Kinetic mechanism of transcription initiation by bacteriophage T7 RNA polymerase. *Biochemistry* **36**(14): 4223-4232

Jiang M, Ma N, Vassilyev DG, McAllister WT (2004) RNA displacement and resolution of the transcription bubble during transcription by T7 RNA polymerase. *Mol Cell* **15**(5): 777-788

Jiang M, Rong M, Martin C, McAllister WT (2001) Interrupting the template strand of the T7 promoter facilitates translocation of the DNA during initiation, reducing transcript slippage and the release of abortive products. *J Mol Biol* **310**(3): 509-522.

Kohlstaedt LA, Wang J, Friedman JM, Rice PA, Steitz TA (1992) Crystal structure at 3.5 Å resolution of HIV-1 reverse transcriptase complexed with an inhibitor. *Science* **256**(5065): 1783-1790

Lescure B, Williamson V, Sentenac A (1981) Efficient and selective initiation by yeast RNA polymerase B in a dinucleotide-primed reaction. *Nucleic Acids Res* **9**(1): 31-45

Ling ML, Risman SS, Klement JF, McGraw N, McAllister WT (1989) Abortive initiation by bacteriophage T3 and T7 RNA polymerases under conditions of limiting substrate [published erratum appears in *Nucleic Acids Res* 1989 Jun 12;17(11):4430]. *Nucleic Acids Res* **17**(4): 1605-1618

Liu C, Martin CT (2001) Fluorescence characterization of the transcription bubble in elongation complexes of T7 RNA polymerase. *J Mol Biol* **308**(3): 465-475.

Liu C, Martin CT (2002) Promoter clearance by T7 RNA polymerase. Initial bubble collapse and transcript dissociation monitored by base analog fluorescence. *J Biol Chem* **277**(4): 2725-2731

Lopez PJ, Guillerez J, Sousa R, Dreyfus M (1997) The low processivity of T7 RNA polymerase over the initially transcribed sequence can limit productive initiation in vivo. *J Mol Biol* **269**(1): 41-51

Ma K, Temiakov D, Anikin M, McAllister WT (2005) Probing conformational changes in T7 RNA polymerase during initiation and termination by using engineered disulfide linkages. *Proc Natl Acad Sci U S A* **102**(49): 17612-17617

Martin CT, Esposito EA, Theis K, Gong P (2005) Structure and Function in Promoter Escape by T7 RNA Polymerase. *Prog Nucl Acid Res Mol Biol* **80**: 323-347

Martin CT, Muller DK, Coleman JE (1988) Processivity in early stages of transcription by T7 RNA polymerase. *Biochemistry* **27**(11): 3966-3974

McAllister WT (1993) Structure and function of the bacteriophage T7 RNA polymerase (or, the virtues of simplicity). *Cell Mol Biol Res* **39**(4): 385-391

McAllister WT (1997) Transcription by T7 RNA polymerase. *Nucleic Acids Mol Biol* **11**: 15-25

Mentesana PE, Chin-Bow ST, Sousa R, McAllister WT (2000) Characterization of Halted T7 RNA Polymerase Elongation Complexes Reveals Multiple Factors that Contribute to Stability. *J Mol Biol* **302**: 1049-1062

Milligan JF, Groebe DR, Witherell GW, Uhlenbeck OC (1987) Oligoribonucleotide synthesis using T7 RNA polymerase and synthetic DNA templates. *Nucleic Acids Res* **15**(21): 8783-8798

Moroney SE, Piccirilli JA (1991) Abortive products as initiating nucleotides during transcription by T7 RNA polymerase. *Biochemistry* **30**(42): 10343-10349

Mukherjee S, Briebe LG, Sousa R (2002) Structural transitions mediating transcription initiation by T7 RNA polymerase. *Cell* **110**(1): 81-91

Mukherjee S, Briebe LG, Sousa R (2003) Discontinuous movement and conformational change during pausing and termination by T7 RNA polymerase. *Embo J* **22**(24): 6483-6493

Muller DK, Martin CT, Coleman JE (1988) Processivity of proteolytically modified forms of T7 RNA polymerase. *Biochemistry* **27**(15): 5763-5771

Place C, Oddos J, Buc H, McAllister WT, Buckle M (1999) Studies of contacts between T7 RNA polymerase and its promoter reveal features in common with multisubunit RNA polymerases. *Biochemistry* **38**(16): 4948-4957

Rong M, Durbin RK, McAllister WT (1998) Template strand switching by T7 RNA polymerase. *J Biol Chem* **273**(17): 10253-10260

Schroeder LA, deHaseth PL (2005) Mechanistic differences in promoter DNA melting by *Thermus aquaticus* and *Escherichia coli* RNA polymerases. *J Biol Chem* **280**(17): 17422-17429

Song H, Kang C (2001) Sequence-specific termination by T7 RNA polymerase requires formation of paused conformation prior to the point of RNA release. *Genes Cells* **6**(4): 291-301.

Sousa R, Chung YJ, Rose JP, Wang BC (1993) Crystal structure of bacteriophage T7 RNA polymerase at 3.3 Å resolution. *Nature* **364**(6438): 593-599

Sousa R, Rose J, Wang B (1994) The thumb's knuckle. Flexibility in the thumb subdomain of T7 RNA polymerase is revealed by the structure of a chimeric T7/T3 RNA polymerase. *J Mol Biol* **244**(1): 6-12

Stano NM, Patel SS (2002) The intercalating beta-hairpin of T7 RNA polymerase plays a role in promoter DNA melting and in stabilizing the melted DNA for efficient RNA synthesis. *J Mol Biol* **315**(5): 1009-1025

Steitz TA (1999) DNA polymerases: structural diversity and common mechanisms. *J Biol Chem* **274**(25): 17395-17398

Straney DC, Crothers DM (1987a) Comparison of the open complexes formed by RNA polymerase at the *Escherichia coli* lac UV5 promoter. *J Mol Biol* **193**(2): 279-292

Straney DC, Crothers DM (1987b) A stressed intermediate in the formation of stably initiated RNA chains at the *Escherichia coli* lac UV5 promoter. *J Mol Biol* **193**(2): 267-278

Tahirov TH, Temiakov D, Anikin M, Patlan V, McAllister WT, Vassilyev DG, Yokoyama S (2002) Structure of a T7 RNA polymerase elongation complex at 2.9 Å resolution. *Nature* **420**(6911): 43-50

Tang GQ, Bandwar RP, Patel SS (2005) Extended upstream A-T sequence increases T7 promoter strength. *J Biol Chem* **280**(49): 40707-40713

Temiakov D, Montesana PE, Ma K, Mustaev A, Borukhov S, McAllister WT (2000) The specificity loop of T7 RNA polymerase interacts first with the promoter and then with the elongating transcript, suggesting a mechanism for promoter clearance. *Proc Natl Acad Sci U S A* **97**(26): 14109-14114

Temiakov D, Patlan V, Anikin M, McAllister WT, Yokoyama S, Vassilyev DG (2004) Structural basis for substrate selection by t7 RNA polymerase. *Cell* **116**(3): 381-391

Theis K, Gong P, Martin CT (2004) Topological and Conformational Analysis of the Initiation and Elongation Complex of T7 RNA Polymerase Suggests a New Twist. *Biochemistry* **43**(40): 12709-12715

Újvári A, Martin CT (1996) Thermodynamic and kinetic measurements of promoter binding by T7 RNA polymerase. *Biochemistry* **35**(46): 14574-14582

Yin YW, Steitz TA (2002) Structural basis for the transition from initiation to elongation transcription in T7 RNA polymerase. *Science* **298**(5597): 1387-1395

Yin YW, Steitz TA (2004) The structural mechanism of translocation and helicase activity in T7 RNA polymerase. *Cell* **116**(3): 393-404

CHAPTER 3

Site Specific Labeling of T7 RNA Polymerase

3.1 Fluorescence Resonance Energy Transfer Overview:

Förster resonance energy transfer (FRET) is widely used in biological and biomedical research as a reporter method. FRET is a common and most sensitive analytical tool for the study of reaction kinetics and molecular conformations, association and separations in the 1- 10 nm range. The current advances in fluorescence microscopy and development of new fluorescent probes makes FRET a powerful technique for studying molecular interactions inside living cells with improved spatial and temporal resolution, distance range and sensitivity. FRET is one of the most developed and promising techniques to identify the binding and interaction of proteins, lipids, enzymes, DNA and RNA in vivo and in vitro.

FRET involves a long-range dipole-dipole interaction between donor and acceptor molecules. The donor molecule excited by a photon, relaxes back to its ground state with a non-radiative transfer of energy by dipolar interaction resulting in excitation of the acceptor molecule. If the absorption spectra of the acceptor and donor molecules overlap, this can result in an indirect excitation of acceptor molecule. The efficiency of transfer (E) is expressed as:

$$E=R_0^6/(R_0^6 + R^6)$$

Where R_0 is the Forster distance at which 50% of the energy transfer takes place and R is the distance between donor and acceptor molecules. We can see from the equation that the transfer efficiency depends on distance (dos Remedios & Moens, 1995; Gohlke et

al, 1994; Wu & Brand, 1994). The actual R_0 value must be determined under experimental conditions because it depends upon the relative angular orientations of donor and acceptor transition movements, the overlap integral, and the quantum yield of donor. FRET studies involve a thoughtful selection of the donor-acceptor pair. The R_0 values could be a deciding factor here. A pair should be chosen that has a R_0 value close to the expected distances before and after the structural change. The simple rule for FRET to be effective is that the distance R between donor and acceptor should lie in the range of $0.5 R_0 < R < 1.5 R_0$ (Clegg, 1992; Sapsford et al, 2006). Fluorescein and rhodamine dyes have been widely used to analyze macromolecular structures and other interactions (Klostermeier & Millar, 2001; Lorenz et al, 2002; Ota et al, 1998; Parkhurst et al, 2001). The adapted figure from Sapsford et al., 2006, clearly shows that there is a considerable spectral separation between the emission of rhodamine and the emission of fluorescein relative to other fluorophore pairs. The same (Fluorescein and Rhodamine; $R_0 = 45 \text{ \AA}$) fluorophore pair was used by Turingan et al., 2007, demonstrating the difference between two proposed models for the structural rearrangement of T7 RNA polymerase in the transition from initiation to elongation. In this work the downstream DNA was modeled in the initiation complex and then various DNA:DNA FRET distances were measured to precisely map the downstream DNA in the initiation and initiating (with 3 base transcript) complexes (Liu & Martin, 2001b; Tahirov et al, 2002; Turingan et al, 2007a; Turingan et al, 2007b; Yin & Steitz, 2002). The initiation (+3) complex appears to be identical to an elongation complex, both in terms of the size of the transcription bubble and positioning of the downstream duplex DNA. Another similar study to differentiate the two transition model based on FRET concluded that the study

supports the shift model in which transition from an initial translation of the N-terminal platform of T7 RNA polymerase away from the C-terminal fixed domain maintains the specificity loop interactions necessary for establishing the stability required to retain promoter contacts (Gong et al, 2004; Liu & Martin, 2002). As the polymerase steps forward, the N-terminal domain moves away from the C-terminal domain resulting in loss of specificity loop contacts and weakening of promoter contacts. Finally, the promoter contacts are lost, which then allows the right handed 220° rotation of the N-terminal domain. This study supports our previously proposed model for the transition, based on topological constraints (Theis et al, 2004).

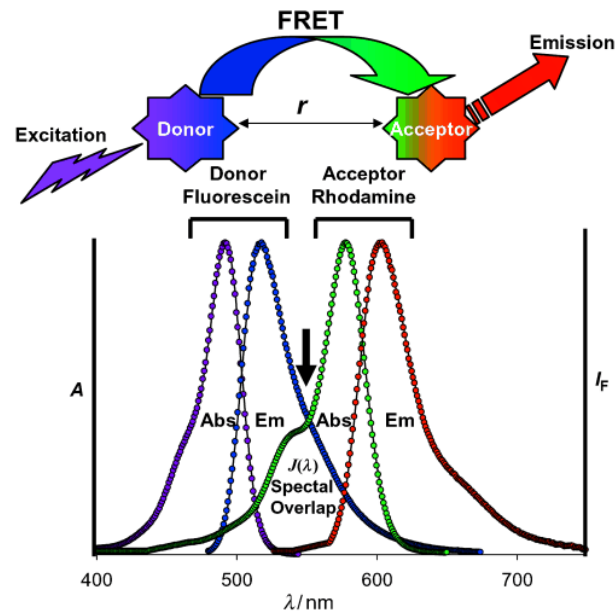


Figure 3.1. Schematic presentation of FRET between donor and acceptor.

When a light source excites the donor, the excited donor transfers energy nonradiatively to its neighboring acceptor molecule. This transfer is dependent on the distance r that separates the donor and acceptor molecules. The acceptor then emits energy either by fluorescence or nonradiative pathways. Both absorption (Abs) and emission (Em) profiles of fluorescein and rhodamine are shown and are plotted as A (normalized absorption) or I_F (normalized fluorescence intensity) versus wavelength in nm (λ/nm). Fluorescein's $\lambda_{exc\ max}$ is about 490 nm and $\lambda_{em\ max}$ is about 515-520 nm and that of rhodamine's $\lambda_{exc\ max}$ is about 565 nm and $\lambda_{em\ max}$ is about 580-585 nm. The spectral overlap between the emission spectrum of fluorescein and the absorption spectrum of rhodamine is also shown. [Reprinted from (Sapsford et al., 2006)]

3.2. SITE-SPECIFIC LABELING OF T7 RNA POLYMERASE:

DNA-to-DNA FRET has allowed mapping the changes that occur before promoter release. Our next goal is to follow predicted motions after promoter release. In order to observe movement of the rotating domain, we need to label it directly. In this case, we will have one probe on the downstream DNA as before and another probe at position 94 in the rotating N-terminal platform of T7 RNA polymerase.

DNA and RNA can be labeled easily postsynthetically since the fluorophore and other probes can be incorporated into the modified bases and then used during the synthesis of DNA/RNA (using nucleotide phosphoramidite chemistry). On the other hand, protein labeling can be challenging and complicated because of numerous amino groups and conjugation will not be specific, as required for FRET. The thiol specific labeling using maleimide chemistry can be helpful in this regard, but the presence of multiple cysteines could be a problem (Sapsford et al, 2006). T7 RNA polymerase has 12 native cysteine residues, 5 buried and 7 surface exposed. Site specific labeling in this case is a challenging task.

Recently, Esposito and Martin have successfully crosslinked promoter DNA to the 94 position which is near the promoter binding site at position -17, using A94C mutant T7 RNA polymerase. The close proximity of the sulfhydryl group incorporated at position -17 in the template strand allows the covalent crosslinking to the 94C position of the A94C mutant T7 RNA polymerase, even in the presence of other cysteines. The activity of the complex under reducing condition was not affected by the mutation and thiol modification of the DNA (Esposito & Martin, 2004a). We used a similar approach to deliver a fluorescent probe to T7 RNA polymerase at position 94.

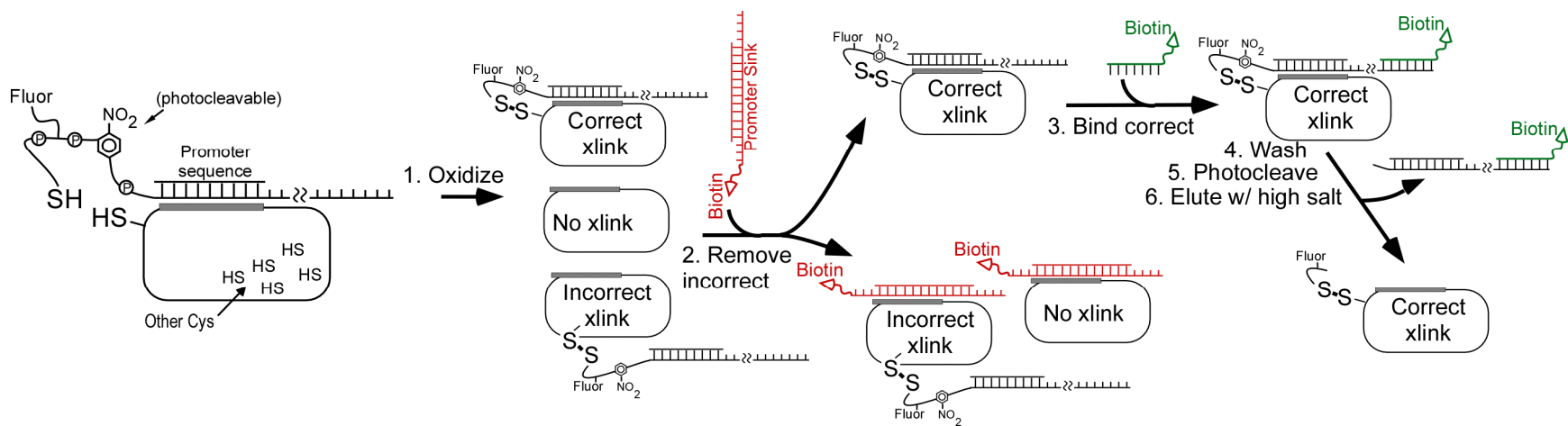


Figure 3.5: Scheme for site-specifically labeling the protein.

Binding of promoter DNA is used to localize a reactive sulfhydryl near an engineered Cys in the protein, as shown in Figure 3.5. Crosslinking of the construct bound to the promoter site occludes binding to other promoter DNA. In step (2), protein containing incorrect crosslinks is bound to immobilized (other) sink DNA. Remaining (correct) complex in the supernatant is then bound to a second solid support containing an oligonucleotide complementary to the downstream ssDNA, washed, photolyzed, and then eluted with high salt.

We have recently developed this approach for site-specific delivery of a fluorophore, exploiting the crosslinking of DNA to a newly engineered Cys in the enzyme with all 12 native cysteines. The approach involves using the template strand tethered with a photocleavable spacer (PC spacer), followed by the fluorophore which is then followed by a -sulfhydryl at 3' end (as shown in Fig. 3.5). Annealing of this under reducing conditions to prevent self crosslinking with non-template DNA (-17 to -5) will create a partial single stranded (pss) labeled DNA. Addition of the enzyme in excess to this pss labeled DNA should result in formation of the promoter bound complex with little non-specific binding to the protein. As the complexes are under reducing conditions, these should not form any crosslinked complexes. On removal of DTT, we would expect crosslinked complexes to form, as in our earlier study (Esposito et. al., 2004).

In recent experiments, DTT was removed by washing with fluorescence buffer (FB) and spinning the reaction mixture through a YM-10 size exclusion column. Uncrosslinked DNA should pass through the column, leaving behind the crosslinked complexes and unlabeled enzyme.

The complexes were then allowed to oxidize by leaving the lid of the eppendorf tube open to air on an ice bath or at 4°C. Additionally, oxidized glutathione (GSSG) could be added (for 30-45 min.) to further facilitate the crosslinking process. In addition to correct crosslinked complexes, we expect to have non-specific crosslinked complexes and free protein in the tube. Non-specific crosslinked complexes and free protein would be removed by binding to a biotinylated pss promoter sink (figure 3.6, the design shown in figure 3.5 at 2nd step). If we still have non-specific crosslinked complexes, we would separate the correct crosslinked complexes by a 14 base long biotinylated non-template

DNA strand complementary to the downstream DNA sequence of the template strand ($T_m = 71.4^\circ\text{C}$). After washing the correct crosslinked complexes with buffer, these would be illuminated with 365 nm UV light, which will cleave the PC spacer at the nitrophenyl ring. The released, labeled protein can then be eluted with a high salt buffer with the enzyme fluorescently labeled at the target Cys (i.e. engineered Cys at 94 position).

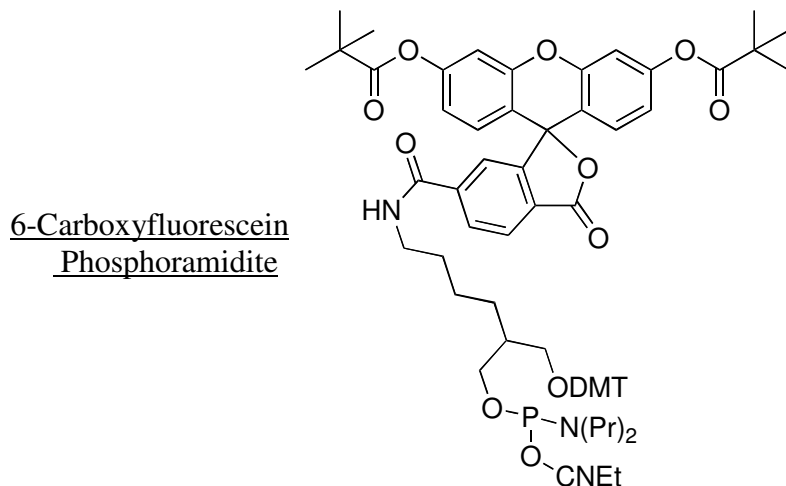


Figure 3.6: DNA constructs used for bead pull down assay

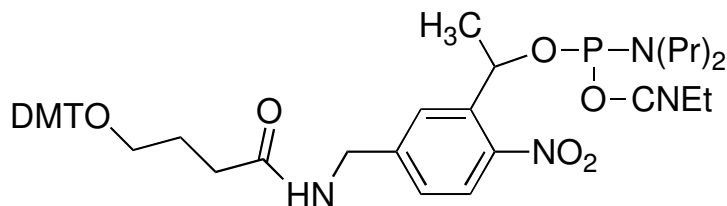
The nontemplate strand (red) with biotin (B) placed at the 3' end, used to fish out the correctly labeled crosslinked complexes than non specific labeled complexes.

As shown in previous work of thiol crosslinking of DNA to the A94C mutant, properly crosslinked complexes are resistant to challenge with a competing promoter sink assay. The sink is a tight binding, but non transcribing DNA construct. The idea is that when protein falls off from the DNA, the sink will replace the other DNA construct because of its more tight binding to the promoter and no transcription will be observed, but if DNA is crosslinked to the protein, the sink cannot replace the DNA and transcription from the crosslinked DNA will be observed. Preliminary results do show crosslinking of this species to the A94C mutant (12 native plus 1 engineered Cys) and at least a population of the enzyme (crosslinked complexes) shows transcription in the presence of inhibiting levels of the promoter sink. From the level of transcription, we estimate more than 50% correct crosslinking of the DNA which is limiting under current conditions. Wild type enzyme (A94) also labels under these conditions as measured by fluorescence in an SDS gel, but the labeled complex is fully inhibited by sink as

expected. Thus, other cysteines are labeling and we suspect that this is due to nonspecific DNA binding.



1-Dimethoxytrityloxy-2-(6-carboxy-(di-O-pivaloyl-fluorescein)-4-aminobutyl)-propyl-3-O-(2-cyanoethyl)-(N,N-diisopropyl)-phosphoramidite
Molecular Formula: $C_{68}H_{78}N_3O_{13}P$
Molecular Weight: 1176.35



PC Spacer Phosphoramidite

[4-(4,4'-Dimethoxytrityloxy)butyramidomethyl]-1-(2-nitrophenyl)-ethyl]-2-cyanoethyl-(N,N-diisopropyl)-phosphoramidite
Molecular Formula: $C_{43}H_{53}N_4O_8P$
Molecular Weight: 784.88

Figure 3.7. Structures of 6-carboxyfluorescein phosphoramidite and the photocleavable (PC) spacer phosphoramidite (Glen Research)

3.3 Preliminary Results:

DNA and protein were incubated in a 1:4 molar ratio to form binary complexes in the presence of DTT (dithiothreitol; 12.85 mM) to avoid the formation of DNA dimer and protein:protein crosslinking. Oxidation follows after complete removal of dithiothreitol (DTT) with air oxidation and/or addition of oxidized glutathione. Along with mutant (A94C), wild type (WT) T7 RNA polymerase is used as a control in all the assays. In this work, we used the “sink-challenge” technique described in the materials and method. The sink is a pss DNA construct forming a non-transcribing stem loop hairpin.

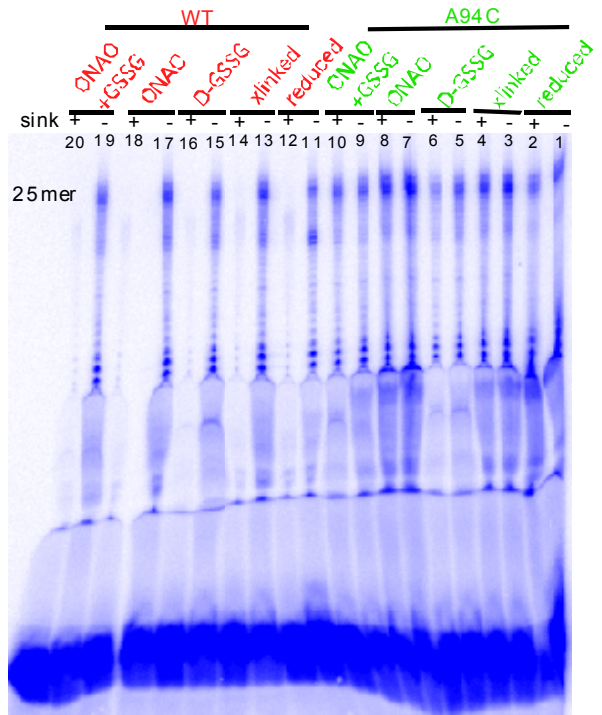


Figure 3.8. The transcription assay on wild-type (WT) and A94C mutant T7 RNA polymerase complexes to assess the formation of crosslinked complexes.

The reduced. from right denote the reduced condition, xlinked denote cross linked complexes just after removing DTT, D-GSSG denote the direct addition of oxidized glutathione after removing DTT, ONAO-GSSG denote the overnight air oxidation followed by oxidized glutathione addition. The + and - denote presence and absence of sink DNA, respectively.

The presence of a photocleavable linker and fluorescent probe on DNA does not affect transcription. Air oxidation followed by the addition of oxidized glutathione pushed the complexes to further oxidation, consistent with earlier reported data (Esposito & Martin, 2004a). As reported by Esposito and Martin, 2004, the correctly crosslinked complexes (A94C mutant complexes) are resistant to a 20 fold excess of sink DNA whereas WT complexes (uncrosslinked) are displaced by the sink DNA. The next step is to isolate the nonspecific crosslink complexes from the correct crosslinked complexes by using the bead pull down assay explained in figure 3.5, step 2. The supernatant left behind from the A94C complexes ideally should contain all specific crosslinked complexes, but there might be some non-specific complexes too. Whereas in case of WT complexes, all complexes should be pulled down by the beads and we should see no transcription (Figure 3.9).

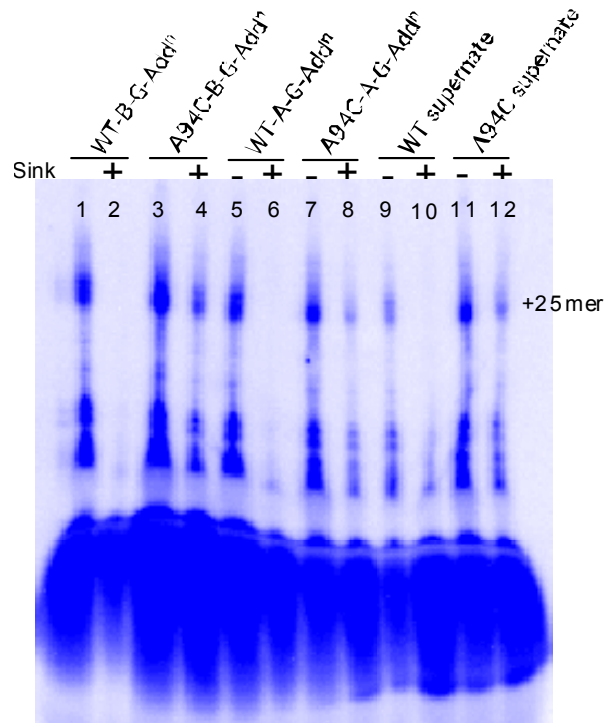


Figure 3.9: Transcribing complexes (Correct crosslinked; resistant to sink) after first bead pull down assay.

From left WT-B-G-Addⁿ and A94C-B-G-Addⁿ denote – WT and A94C complexes before glutathione addition respectively, WT-A-G-Addⁿ and A94C-A-G-Addⁿ denote – WT and A94C complexes after glutathione addition respectively, supernatant (after pulling out free and the non-specific crosslinked complexes) contains correctly crosslinked complexes.

To attain our goal of specific labeling using A94C mutant, we proposed to alter the length of the PC linker and the positioning of the PC spacer on the upstream DNA for a more optimal disulfide linkage formation at position 94 in the protein. We will also try to use a mutant that has 7 surface cysteines deleted, prepared by Sousa et al. (Mukherjee et al, 2002; Sousa, 2003) (plasmid for this mutant protein was kindly supplied by Rui Sousa). By engineering a cysteine at position 94 in this mutant, we would expect to see an increased level of specific crosslinked complexes. Assuming that, this engineered protein will be an active protein in terms of transcription to demonstrate the efficiency of labeling and later for the FRET measurement.

3.4 An alternate route of site-specific protein labeling:

Most methods to produce labeling exploit the nucleophilicity of either amines (lysine side chain and the N-terminus) or thiols (cysteine side chain) on the protein surface. Cysteine labeling is typically more specific than amine labeling as the cysteine is less abundant in proteins and a single cysteine can often be added by site-directed mutagenesis without affecting the function of the protein. This cysteine labeling in turn would allow us to label the protein site-specifically with a fluorophore. Incorporation of the fluorophore enables the study of changes in the conformation of complexes by fluorescence or FRET measurements. A change of protein conformation should, by definition, result in a change of some interatomic distances within the protein molecule. Fluorescence donor and acceptor probes placed at appropriate sites in the protein should then be able to report such conformational changes in FRET signal. The ability to introduce the probes into desired locations within the protein is crucial for the successful

outcome of such experiments and is usually the most challenging part of designing FRET experiments to study conformational changes in a protein.

In 1994, Dawson et. al. first introduced a method of native chemical ligation (NCL) (see appendix D) for ligating a synthetic peptide segment to generate full protein. This technique is limited by the size of the synthetic peptide segment and has not been extended to the synthesis of proteins beyond 15 KDa. T7 RNA polymerase is a 99 KDa protein, which is beyond the range of this technique.

An extension of the “native chemical ligation”, approach that can overcome the size limitation is “expressed protein ligation”, in which a small synthetic sequence is chemically ligated to a much larger recombinant protein fragment. The details of the process are discussed below.

3.4.1 Expressed Protein Ligation:

In so called “native chemical ligation” an N-terminal Cys containing peptide and α -thioester group containing peptide for use in native chemical ligation are generated solely through chemical synthesis, a technically demanding process that imposes certain size constraints on the technique. One way to overcome this size limitation is to chemically ligate small synthetic sequences to much larger recombinant protein fragments. Protein splicing, the process in which a protein undergoes an intramolecular rearrangement resulting in the extrusion of an internal sequence (intein) and the joining of the lateral sequences (exteins), has been shown to involve the intermediacy of a thioester (Xu & Perler, 1996). A mutant version of the splicing protein has been demonstrated to be defective in completion of the splicing reaction but still capable of thioester intermediate formation. The commercially available pCYB vectors for *Escherichia coli* protein

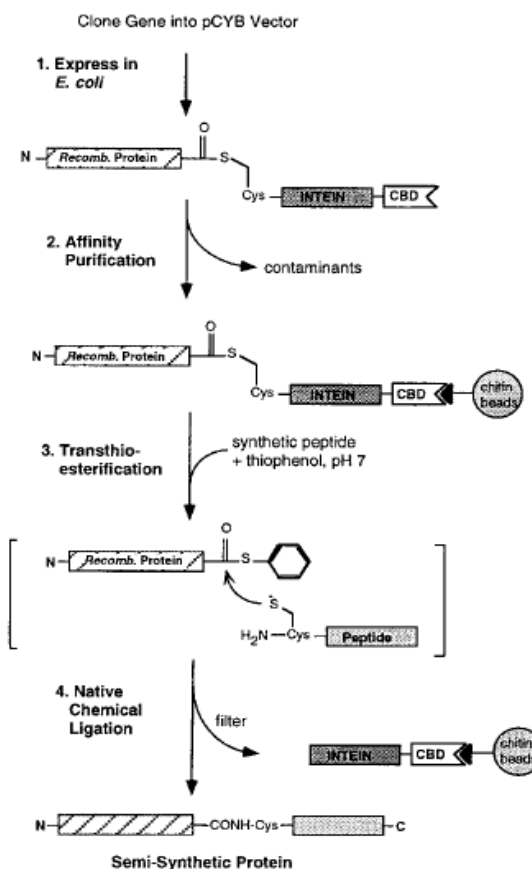


FIG. 3.10. The principle of expressed protein ligation.

In the first step, the gene or gene fragment is cloned into the commercially available PCYB2-IMPACT vector (New England Biolabs) by using the *NdeI* and *SmaI* restriction sites. This cloning strategy results in the addition of a Pro-Gly appended to the native C terminus of the protein of interest. The presence of a C-terminal glycine has been shown to accelerate native chemical ligation and thus reduces the chance of side reactions. After expression and affinity purification of the fusion protein by binding to the chitin resin, the chemical ligation step is initiated by incubating the resin-bound protein with thiophenol and synthetic peptide in buffer. This results in the *in situ* generation of a highly reactive phenyl thioester derivative of the protein that then rapidly ligates with the synthetic peptide to afford the desired semisynthetic protein. (figure is reprinted from (Muir et al, 1998).

expression result in the generation of α -thioesters where a protein of interest can be expressed in frame fused with an intein-chitin binding domain (CBD) sequence (Muir et al, 1998). In the standard experiment, the protein of interest is cleaved from the intein-CBD with DTT or 2-mercaptoethanol by a transthioesterification reaction while the chimera is bound to a chitin column. But Muir found that its possible to intercept the α -thioester with a synthetic peptide rather than DTT, thereby generating a semisynthetic protein (Figure 3.10) containing a chemoselectively ligated synthetic peptide sequence. The approach “expressed protein ligation” is very simple, involving a single chemical step, and effectively unites the field of synthetic peptide chemistry and recombinant protein biotechnology.

The ability to insert synthetic peptides into recombinantly expressed proteins opens powerful new pathways in protein engineering and complement existing approaches for introducing unnatural amino acids and biophysical probes into large proteins. The biosynthetic strategy (Graham J. Cotton, 1999) outlined in Figure 3.11 extends this approach by allowing a peptide insert, containing both an N-terminal cysteine residue and an α -thioester moiety, to be inserted between two recombinant proteins containing complementary reactive groups at their N- or C-termini.

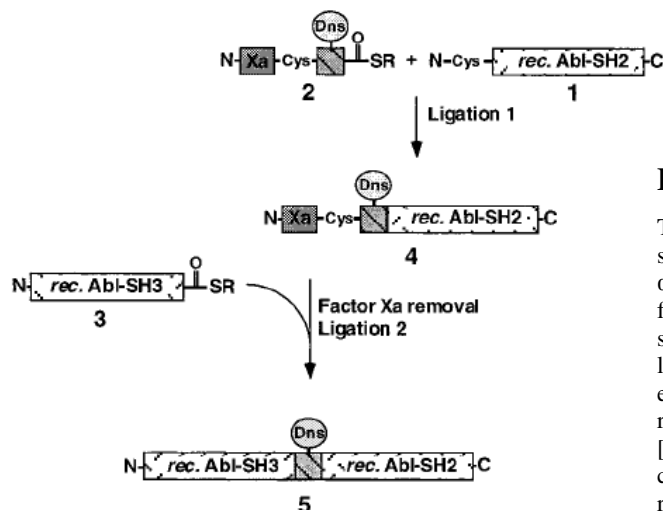


Fig. 3.11. Sequential ligation strategy.

The first step involves native chemical ligation of the synthetic peptide GKIEGR-CK(Dns) Gpropionamide α -thioester¹¹ to the recombinant N-terminal Cys fragment, Abl-[C121]SH2. After purification the pro-sequence RGKIEGR (Xa) is removed from the ligation product by treatment with factor Xa. This exposes a N-terminal cysteine residue which is then reacted with the recombinant thioester fragment, Abl-[G¹²⁰]SH3-ethyl α -thioester,¹³ in a second native chemical ligation step. (Figure is reprinted from reference (Graham J. Cotton, 1999)).

Key to this sequential ligation process was the reversible N α -protection of the cysteine residue in the central peptide, which allows the two ligation reactions to be performed in a controlled, directed fashion. A mild enzymatic N α -protection strategy was employed that involved appending the short propeptide, RGKIEGR, to the N-terminal Cys of the central peptide. Model studies indicated that this peptide-protecting group prevented self-ligation, yet could be cleanly removed at pH 7.5 by treatment with the protease factor Xa (Erlanson et al, 1996). Note, this enzymatic N α -protection strategy is compatible with both the chemical synthesis and biosynthesis of peptides and proteins.

3.4.2 Protein *trans*-splicing (PTS):

Protein splicing is a post-translational process in which a precursor protein undergoes a self-catalyzed intramolecular rearrangement that results in the removal of an internal protein domain, termed an intein, and the ligation of the two flanking polypeptides, referred to as the N and C exteins. Inteins are autocatalytic and some are remarkably promiscuous with respect to the sequences of the two flanking exteins (Muralidharan & Muir, 2006). Biochemical studies have revealed the basic chemical steps in protein splicing and have identified the key conserved residues within the intein family required for these steps. Although most protein splicing reactions occur in *cis* and involve intact inteins, split inteins participate in a protein *trans*-splicing reaction. In this process, complementation of the intein fragments precedes the normal splicing reaction (Fig. 3.12). A protein of interest is expressed as an in-frame N- or C-terminal fusion to the mutant intein, which is usually linked to an affinity tag. After purification, the protein of interest can be cleaved off the intein by addition of thiols (C-terminal cleavage, that is, the protein corresponds to the N extein) or by changing the pH and temperature of the solution (N-terminal cleavage, that is, the protein corresponds to the C extein). These intein-based expression systems can be used for the ‘traceless’ purification of recombinant proteins. Notably, these intein fusions provide a convenient route to recombinant proteins containing an N-terminal cysteine or a C-terminal thioester. *Trans*-splicing inteins are commercially available in two types, those that are artificially generated by splitting a normal *cis*-splicing intein and those that are naturally split, the best characterized of which is the Ssp DnaE intein. The key functional difference relates to the affinity of the complementary fragments; the DnaE split intein fragments associate

with high affinity, whereas artificially split intein fragments typically do not. For this reason, the DnaE split intein is preferable for most protein ligation applications *in vitro* and *in vivo*. On the other hand, artificially split inteins are useful for two- and three-hybrid applications as PTS only occurs when the fragments are at high local concentration. Another very useful feature of PTS is that different pairs of split inteins do not cross-react, allowing multiple protein ligation reactions to be performed simultaneously (Schultz, 2005).

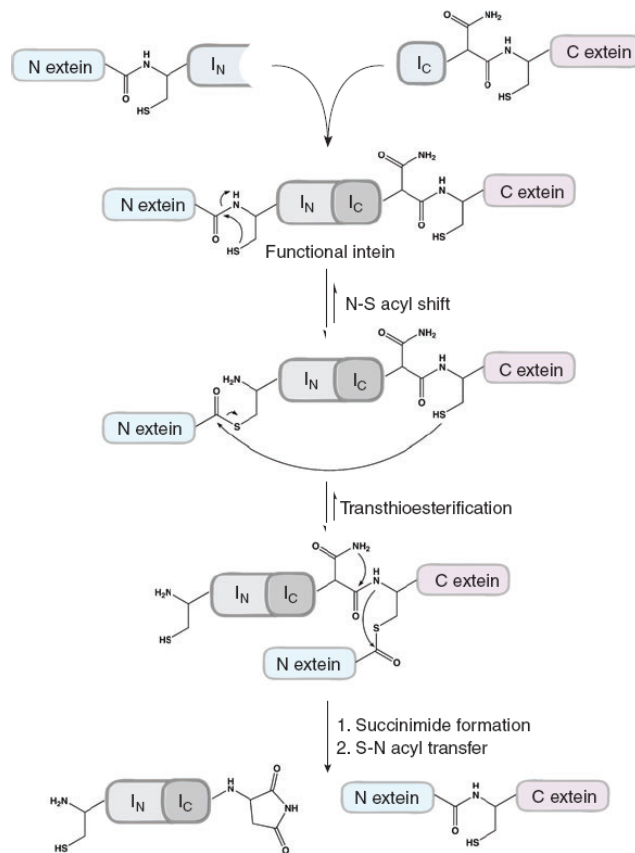


Figure 3.12 Principle of protein *trans*-splicing (PTS).

The two halves of the split intein, labeled as I_N and I_C , associate and fold to form a functional intein. This functional intein can then undergo a pseudo-intramolecular protein splicing reaction, wherein the flanking polypeptides, termed the N and C exteins, are ligated together and the intein excises itself. (Figure is reprinted from reference (Muralidharan & Muir, 2006)).

3.3 Scheme of making recombinant T7 RNA polymerase

Based on the above approaches, we designed the scheme shown in figure 3.13 to label T7 RNA polymerase: First, the N-terminal fragment encoding amino acids 1-264 will be cloned into the pTWIN1 vector which is commercially available and allows a protein of interest to be expressed in frame, fused with an intein-chitin binding domain sequence, and expressed in a bacterial system. The purified protein fragment will be subjected to intein thiolysis generating an α -thioester group at the C-terminus of the protein. As this expressed protein fragment will have only one cysteine (the other two at 125 and 216 have been mutated), it can be directly coupled with fluorophore by maleimide labeling. In the same way, the remaining fragment encoding amino acid 265-883 will be cloned in pTWIN1 vector and expressed in bacterial system. After purification with chitin beads, the protein will be subjected to intein cleavage by change in pH or temperature condition resulting in an N-terminal cysteine for this protein fragment.

The two purified protein fragments, one having the N-terminal cysteine and the other fluorophore labeled protein fragment containing an α -thioester group at the C-terminus will be subjected to “native chemical ligation”, resulting in the full length protein i.e. T7 RNA polymerase labeled with fluorophore.

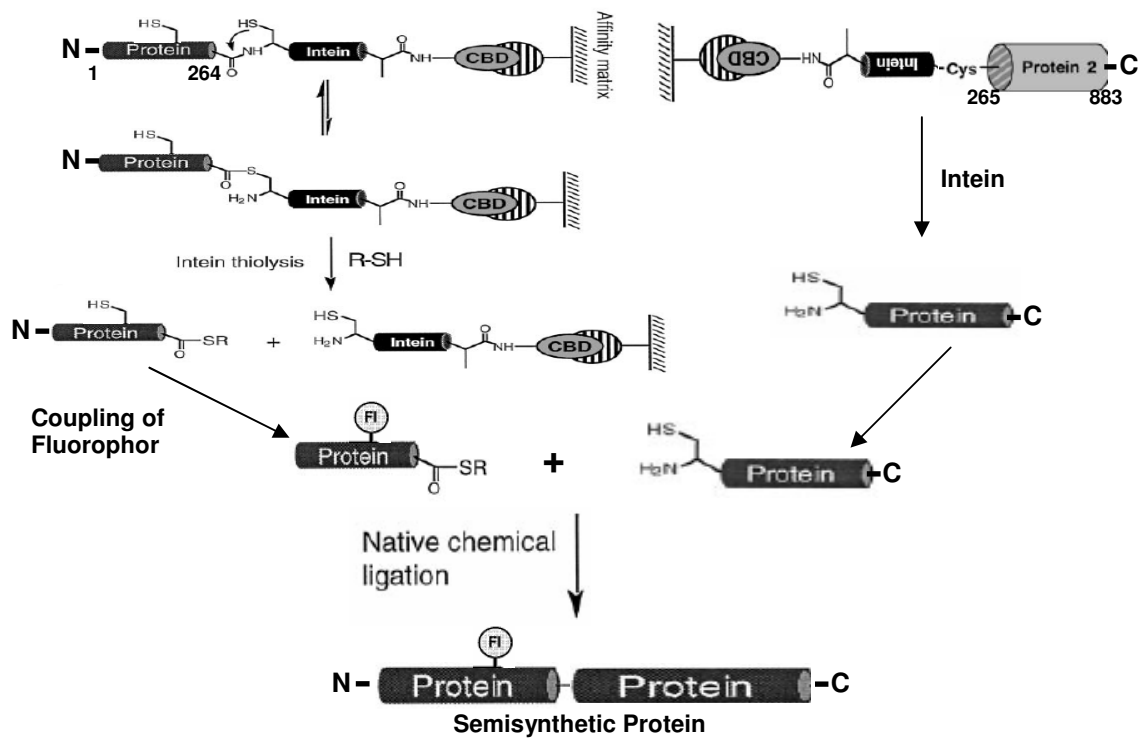


Fig.3.13. Scheme of recombinant protein α -thioesters and expressed protein ligation.

N-terminal platform (residues, 1-264) will be expressed with C-terminal fused intein and C-terminal domain (residues, 265-883) will be expressed with N-terminal fused intein.

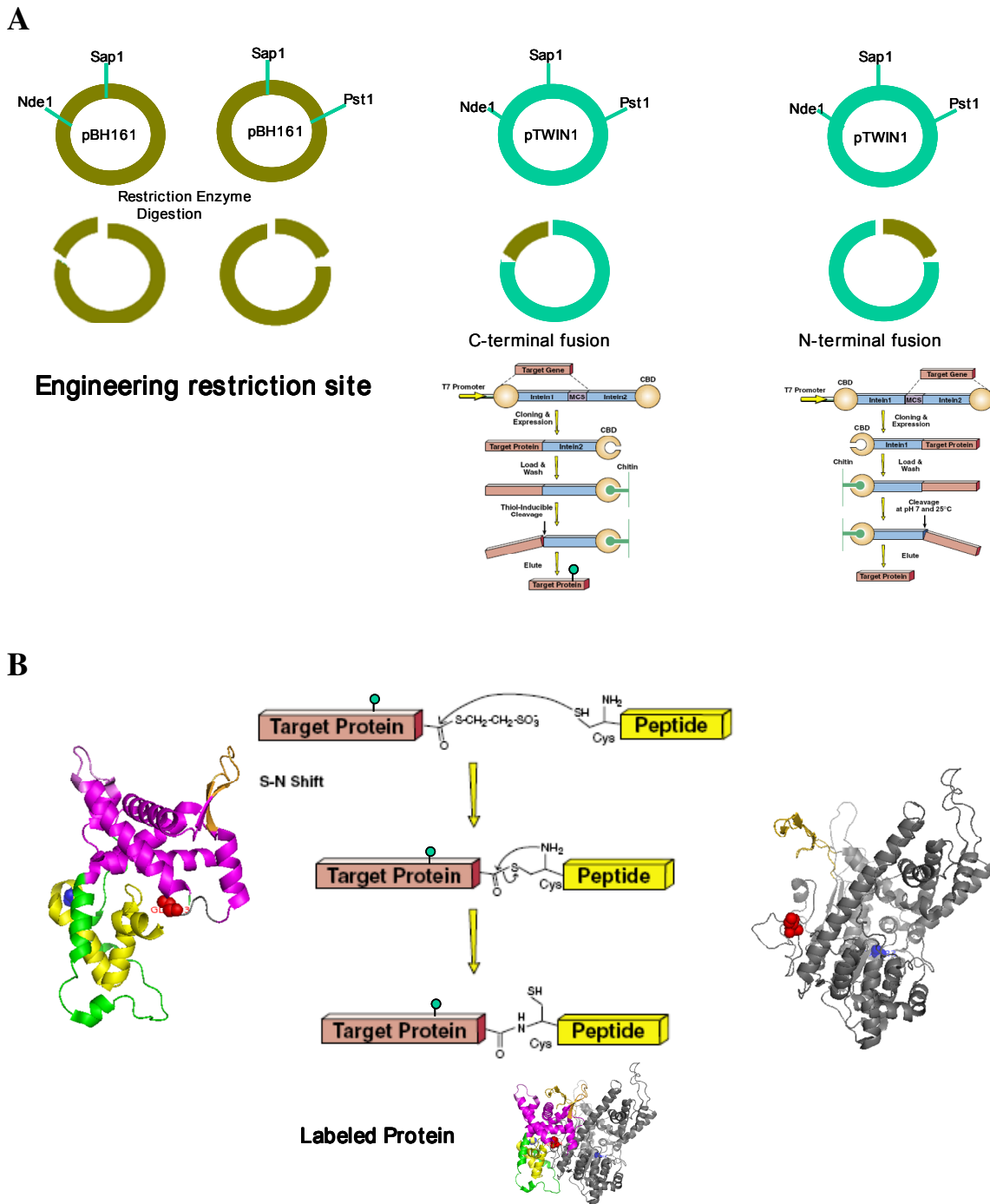


Figure 3.14: A) Schematic presentation of engineering restriction site in pBH161 plasmid and insertion of the fragments of interest in pTWIN vector, B) schematic presentation of protein ligation process to yield recombinant protein.

As explained in the figure 3.14 A, we have engineered the restriction site (i.e. Nde1 & Sap1 in one case and Sap1 & Pst1) in the same pBH161 plasmid. These restriction sites are complementary to the site in the pTWIN vector and will generate protein fragments corresponding to the N-terminal and C-terminal fusion intein sequences. Nde1 and Sap1 site ligation will generate the C-terminal fusion (pTWIN vector) and Sap1 & Pst1 site ligation will generate the N-terminal fusion. The C-terminal fused intein will generate the C-terminal thioester moiety after overexpression of the protein fragment followed by the intein thiolysis. The N-terminal fused intein after lysis will generate the N-terminal cysteine necessary for ligation of the two recombinant protein fragments. As the N-terminal platform of T7 RNA polymerase will have only one cysteine, it will be labeled by the direct addition of fluorophore using thiol chemistry. Finally, both protein fragments will be mixed in an eppendorf tube and the native chemical ligation reaction will take place, producing a complete T7 RNA polymerase with the fluorophore labeled at the desired position. It is possible that ligation may not be 100%, so separation of the ligated protein from the unligated fragments using size exclusion chromatography will be necessary.

3.4 Materials and Methods:

3.4.1 Construction and purification of the mutant (A94C) & WT T7 RNA polymerase

The mutant polymerase was prepared and purified according to the protocol described in the literature (Esposito & Martin, 2004a). An expression vector for His-tagged A94C was prepared in accordance with the protocol provided in the Stratagene QuickChange™ site-directed mutagenesis kit. William McAllister generously provided

the parental plasmid from pBH161/BL21 cells. The primers bearing the cysteine mutation and its complementary sequence were purchased from Integrated DNA Technologies and the resulting plasmids were transformed into BL21 cells.

His-tagged A94C mutant and WT T7 RNA polymerase were over expressed in *E. coli* strain BL21 and purified using Qiagen Ni-NTA column material. The fraction collected from Ni-NTA column were further purified by Toyopearl ion-exchange columns such as CM - 650 M and DEAE - 650 M columns from Tosoh Bioscience. Protein purity was determined by SDS-PAGE gel analysis. The purified proteins were concentrated and dialyzed against 100 mM NaCl, storage buffer pH 7.8 (1.6 mM KH_2PO_4 , 18.2 mM K_2HPO_4 , 50% glycerol and 1 mM Na_2EDTA) and stored at -20°C . Protein concentration was calculated from the measured absorbance at 280 nm using the molar extinction coefficient of $1.4 \times 10^5 \text{ M}^{-1}\text{cm}^{-1}$ (King et al, 1986). Activity was determined by a “transcription assay” described below.

3.4.2 Synthesis and purification of oligonucleotides

All the oligonucleotides (modified or normal) were synthesized (1 μmol scale, tityl off) using phosphoramidite chemistry on a Biosystems Expedite 8909 Nucleic Acid Synthesis System. The PC spacer phosphoramidite (100 μmol), Unilinker and carboxyfluorescein phosphoramidite (50 μmol) were dissolved in 1.0 mL, and 0.5 mL of anhydrous acetonitrile, respectively. While the normal/unmodified promoter nontemplate strand was synthesized in regular standard base columns, the downstream biotinylated nontemplate strand and the template strand for the partially single-strand sink were synthesized on a 3'-biotin column and the promoter template strand on a 3'-thiol modifier

column (amidites and columns were purchased from Glen Research). For the partially single-stranded sink (pss) DNA, the (-22 to -5) sequence of nontemplate strand is 5'-GAAATTAATACGACTCACTATA-3' and the (-27 to +3) sequence of the template strand is 3'-TGAAGCTTTAATTATGCTGAGTGATATCCC-5'. The nontranscribing stem-loop hairpin sink is a single-strand 39-mer DNA with sequence 5'-TATAGTGAGTCGTATTAAGCGAAGCTTAATACGACTCAC-3'. The synthesized oligonucleotides were cleaved from the column and deprotected with concentrated ammonium hydroxide (for the promoter template strand, ammonium hydroxide with 100 mM DTT was used). All oligonucleotides were purified by gel electrophoresis using a denaturing 15% polyacrylamide gel. For the template strands, the fluorescent bands were visualized using a "blue-laser" configuration in the Fuji Imager (Fuji Film FLA-5000) and then excised to isolate from the unlabeled DNA bands. DNA strands were extracted from the gel slices using the Elu-Trap®, ethanol precipitated and dissolved in TE buffer as described in the previous chapter(s).

3.4.3 Synthesis and fluorescent probe labeling of DNA

Oligonucleotides were synthesized (1 μ mol scale, trityl off) using phosphoramidite chemistry on a Biosystems Expedite 8909 Nucleic Acid Synthesis System. Amino-modified Unilinker phosphoramidite (Glen Research) was introduced during the synthesis at selected positions. To ensure that the amine-modified oligonucleotides are free of shorter sequences and of triethylamine and ammonium salts that may interfere with the labeling, purification by gel electrophoresis followed by ethanol precipitation was done. Single-stranded DNA with and without modifications was purified by 15%

polyacrylamide [19:1 (w/w) acrylamide:bisacrylamide]/6 M urea, 0.8 mm thick gel and ran at 55-60 Watts. Oligonucleotides of desired length were excised from the gel and the DNAs were extracted using an electro-separation chamber (Elu-Trap®, Schleicher and Schuell) run at 150 Volts for 3 hours or at 100 Volts for overnight. For the ethanol precipitation, 1 volumes of the extracted pure DNA solution was mixed with 1 μ L volume of linear acrylamide as a carrier, 0.1 volume of 3 M NaOAc and 2.5 volume of cold absolute ethanol. This mixed solution was placed at -80⁰C for about 15 minutes and then centrifuged at 14,000 x g for full 30 minutes inside the 4⁰C delicase. The air-dried DNA pellet was dissolved in the desired volume of TE buffer (10 mM Tris, pH 7.8, 1 mM EDTA) and the concentration determined by UV-Vis absorbance at 253, 259 and 267 nm. These were readily calculated from the weighted sums of the 3 different measured molar extinction coefficients for each base at a particular wavelength (Schick & Martin, 1993). In this case, we used ϵ_{253} , ϵ_{259} , ϵ_{267} values as 344500 M⁻¹cm⁻¹, 375800 M⁻¹cm⁻¹, and 349800 M⁻¹cm⁻¹, respectively.

The procedure for fluorescently labeling these amine-modified oligonucleotides was derived from a combination of the protocols provided by Invitrogen (formerly Molecular Probes) and by Mary Barkley's lab (Case Western University). Labeling was done postsynthetically in 1 M Na₂CO₃ (pH adjusted to 9.5 with HCl) reaction buffer. The aliquoted fluorescent dyes, 5-carboxytetramethylrhodamine succinimidyl ester (Invitrogen) and fluorescein isothiocyanate (Anaspec, Inc.) were initially dissolved in DMSO. Efficient labeling was achieved by mixing a 25-fold molar excess of dye to DNA. The final concentration of Na₂CO₃ in the reaction mix is 200 mM. The labeling was allowed to proceed for 2-3 hours at 37⁰C. Longer incubation times did not result in

any further increase in labeling efficiency. Ethanol precipitation was carried out for all the labeled oligonucleotides. This was done twice for TAMRA-labeled samples since TAMRA has a tendency to adhere nonspecifically to the oligonucleotide (Molecular Probes). The labeled oligonucleotides were further purified by gel electrophoresis using 15-20% polyacrylamide gel electrophoresis. Fluorescent bands were visualized using a UV illuminator box (Fotodyne Incorporated, Model No. 3-3000, Serial No. LTD1-0489-2852) and then excised to isolate from unlabeled DNA bands. The labeled DNA strands were again extracted from the gel slices using the Elu-Trap® and ethanol precipitated. The labeled DNA pellets were rinsed twice with cold 70% ethanol and allowed for quick air-drying. Dissolution of fluorescently labeled DNA strands in TE buffer was done prior to determination of concentration by UV spectroscopy.

3.4.4 Determining corrected single-stranded DNA concentration

The fluorescent dyes have some absorbance at about 260 nm, similar to DNA. The contribution of fluorescent probes to DNA absorbance was subtracted to correctly determine the concentration of labeled DNA strands. To do this, we dissolved both the pure or free dyes in TE buffer and the dye samples conjugated to the DNA and performed a full-UV scan from 220-650 nm. By so doing, we also confirm that conjugation indeed happened. Equation 3.2 gives the corrected absorbance at a particular wavelength (in this case, at 253 nm, 259 nm and 267 nm).

Equation 3.2:

$$A_{\lambda}^{Corrected} = A_{\lambda}^{Obsrvd} - \left(A_{\lambda_{max}^{FITC}}^{Obsrvd} \left(\frac{A_{\lambda}^{FITC}}{A_{\lambda_{max}^{FITC}}^{FITC}} \right)_{PureFITC} + A_{\lambda_{max}^{TAMRA}}^{Obsrvd} \left(\frac{A_{\lambda}^{TAMRA}}{A_{\lambda_{max}^{TAMRA}}^{TAMRA}} \right)_{PureTAMRA} \right)$$

The average was used as the final concentration of the labeled DNA. The labeling efficiency was calculated by getting the molar ratio of dye to DNA.

3.4.5 Preparation of duplex DNA

Complementary strands (1:1 molar concentration) of TAMRA-labeled or unlabeled nontemplate strands and FITC-labeled template strands were hybridized in TE buffer. The annealing was done for 5 minutes at 75⁰C and then slowly cooled to room temperature over about 2-3 hours. Annealed DNA was either stored at -20⁰C or immediately used for purification. Samples were again gel-purified using a 12% native acrylamide slab gel (10 mL total volume contains 3 mL 40% acrylamide, 2 mL of 5X TBE buffer (0.45 M Tris, 0.45 M boric acid and 0.01 M EDTA), 5 mL distilled H₂O, 7.5 μL TEMED and 750 μL of 10% ammonium persulfate) to separate labeled double-stranded DNA from excess (labeled or unlabeled) single-stranded DNA. Fluorescent bands were imaged using a Fuji Imager (Fuji Film FLA-5000). These methods were designed to obtain 100% labeling efficiency.

Ideally, for a long polymer made up of interacting monomers, the overall integrated absorption intensity is equal to the sum of the absorption intensities of the individual monomers. However, this is not often true as can be observed in DNA. The intact double helix absorbs light that is less than that absorbed by the mixture of same monomers. That

is because a transition in one monomer can be influenced by other transitions in its neighbor. The effect can be seen in terms of induced dipole effects. If the dipoles are aligned parallel to each other, there will be mutual repulsion which makes the induction of each dipole by an electric field more difficult. The transition probability will be reduced and the resulting extinction coefficient will be smaller. This hypochromism event occurs in double-stranded DNA. This hypochromism explains why we observe a decrease in the extinction coefficient for duplex DNA versus melted DNA. In determining the corrected concentration of the labeled duplexes, we first obtained the hypochromicity factor, X, which was measured using unmodified and unlabeled template and nontemplate strands before and after hybridization at room temperature for 5, 8, 10 and 15 minutes and also at 75⁰C and then slow cooling to room temperature for 3 hours. Average absorbance results from these different hybridization times showed X=0.435. This average absorbance was taken by averaging the absorbances at 253 nm, 259 nm and 267 nm. Incubation at 75⁰C and then slow cooling to room temperature has the same effect on double-stranded DNA prepared and annealed at room temperature. Equations 3.3-3.6 were used to calculate for the corrected concentration of each the labeled duplexes.

Equation 3.3:
$$A_{259} = X(\epsilon_{template} + \epsilon_{nontemplate})[dsDNA]$$

Equation 3.4:
$$[dsDNA] = \frac{A_{259}}{0.435(\epsilon_{template} + \epsilon_{nontemplate})}$$

Equation 3.5:

$$A_{259}^{Corrected} = A_{259}^{Obsrvd} - \left(A_{\lambda_{max}^{FITC}}^{Obsrvd} \left(\frac{A_{259}^{FITC}}{A_{\lambda_{max}^{FITC}}^{FITC}} \right)_{PureFITC} + A_{\lambda_{max}^{TAMRA}}^{Obsrvd} \left(\frac{A_{259}^{TAMRA}}{A_{\lambda_{max}^{TAMRA}}^{TAMRA}} \right)_{PureTAMRA} \right)$$

Equation 3.6:

$$[dsDNA] = \frac{A_{259}^{Obsrvd} - \left(A_{\lambda_{max}^{FITC}}^{Obsrvd} \left(\frac{A_{259}^{FITC}}{A_{\lambda_{max}^{FITC}}^{FITC}} \right)_{PureFITC} + A_{\lambda_{max}^{TAMRA}}^{Obsrvd} \left(\frac{A_{259}^{TAMRA}}{A_{\lambda_{max}^{TAMRA}}^{TAMRA}} \right)_{PureTAMRA} \right)}{0.435(\varepsilon_{template} + \varepsilon_{nontemplate})}$$

3.4.6 Binding and cross-linked complex formation

A 1:1 molar ratio of template and nontemplate strands were annealed in fluorescence binding buffer (30 mM HEPES (pH 7.8), 25 mM potassium glutamate, 0.25 mM EDTA, 100 mM NaCl and 0.5% glycerol) and freshly prepared 100mM DTT. This 2.6 μ M duplex DNA solution with DTT about 13mM was split into 2 tubes-one for A94C and WT assay. Binary complexes were allowed to form at room temperature for 20-25 minutes. The total volume of each pssDNA:enzyme mixture was 100 μ L with final concentrations of DNA and enzyme equal to 2 μ M and 8 μ M, respectively. During the incubation period, 2 YM-10 columns were pre-rinsed with 100 μ L fluorescence binding buffer and centrifuged for 10 minutes. A 10 μ L aliquot of pssDNA:A94C and pssDNA:WT were taken out for transcription analysis under reducing conditions, and the

rest was placed in these YM-10 columns and to each tube, 400 μL of fluorescence binding buffer was added. The tubes were spun down to dead stop volume of about 40 μL at 14,000 rpm for 2 full 30-minute spins inside the 4⁰C-delicase. To the 40 μL retentate, 460 μL of buffer was added with pipetting to wash the sides of the column for any sticking protein but careful enough not to touch the membrane. The tubes were again spun down to dead stop volume of about 40 μL at 14,000 rpm for 2 full 30-minute spins inside the 4⁰C-delicase. This washing and spinning were done 2 more times to ensure that all DTT has been washed off. Then, the collected 40 μL retentate was transferred into a new tube by inverting the YM-10 column cup and spinning down for about 30 seconds. The YM-10 cup was rinsed with 50 μL fluorescence binding buffer and the wash solution was combined with the retentate. The resulting complex was allowed to air oxidize for 30 minutes and took a 10 μL aliquot for transcription analysis under “mild” oxidizing condition. To the remaining solution, 2 μL of 100 mM oxidized glutathione was added and oxidation was allowed to occur for at least 30 minutes (an aliquot was taken at this stage for transcription under oxidizing conditions) prior to isolating the complex by a bead pull down assay. The complexes were stored at -20⁰C.

3.4.7 Streptavidin-bead pull down assay

100 μL of DYNAL® Dynabeads® M-280 Streptavidin (Dynal Inc.) was obtained and the supernate was removed by placing the tube in a provided magnet. The beads were washed 3x with 1x B&W buffer (diluted from 2 x B&W buffer which contains 10mM Tris-HCl, pH 7.5; 1 mM EDTA and 2.0 M NaCl). After removal of the supernatant in the last wash, 50 μL of 100 μM biotinylated pssDNA sink and 50 μL of 2 x B&W were

added. Streptavidin bead:biotinylated DNA mixture was incubated for about an hour while spinning at room temperature so as not to allow the beads to settle down the tube and consequently, ensures maximum binding capacity. The supernatant was removed and replaced with 100 μL of fluorescence binding buffer and then washed twice. After the second wash, the samples were divided into 2 tubes containing 50 μL mixture. The beads were pulled down and the supernatant was discarded. To each tube, 50 μL of the cross-linked complexes of A94C and WT and 50 μL of fluorescence binding buffer were added. The samples were allowed to incubate at room temperature for 15 minutes. The beads were again pulled down and the supernatant was removed which, ideally, should contain 100% specific cross-links. A 10 μL aliquot from this bead-isolated complex was used for transcription analysis under oxidizing condition.

Equal volumes of downstream nontemplate strand (~40-folds excess of the initial concentration of pssDNA in the binary complex), which has a biotin-tagged at the 3'-end in 1x B&W and pre-washed Dynabeads, were incubated for about 30 minutes at room temperature and the B&W buffer was replaced with the same volume of fluorescence binding buffer. The tubes were again split into 2 and then pulled down to discard the supernatant. To each tube, bead-isolated complex was added and incubated for 30 minutes prior to addition of fluorescence binding buffer to meet the fluorimeter cuvette capacity.

3.4.8 Transcription and sink-challenge assay

Transcription reactions were performed in a total volume of 10 μL (5 μL of complex, 4 μL of either fluorescence binding buffer or promoter sink and 1 μL of NTP-

mix) at 37⁰C for 5 minutes and quenched with an equal volume of stop solution (90% formamide, 40 mM Na₂EDTA, 0.02 (w/v) bromophenol blue). Reactions were initiated by the addition of GACU-mix labeled with [α -³²P]GTP (Perkin Elmer Life Sciences). Final concentrations of each nucleoside triphosphates are 400 μ M.

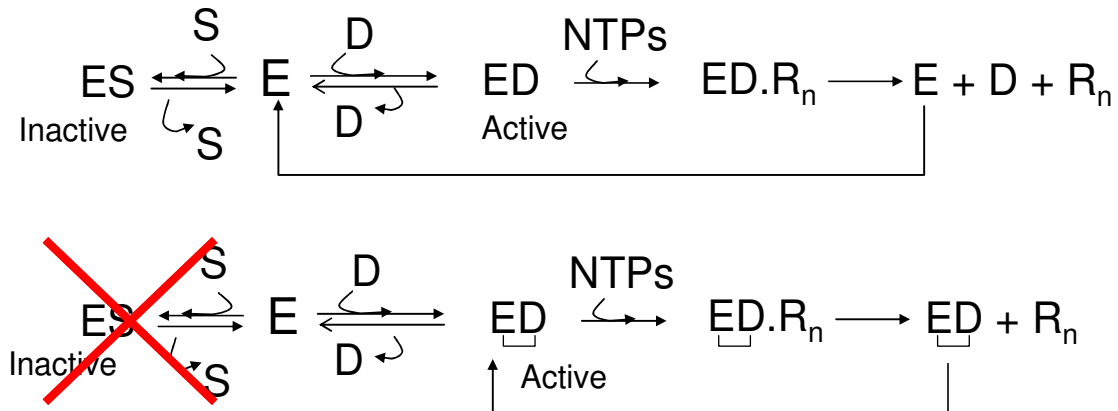


Figure 3.15 Schematic presentation of sink challenge assay.

RNA transcripts were visualized by electrophoresis using a 0.4mm thin gel, 20% polyacrylamide [19:1 (w/w) acrylamide:bisacrylamide]/7M urea and ran at 55Watts for about 2 hours. The gel was scanned using a Fuji PhosphorImager FLA-5000.

3.5 References:

- Borukhov S, Lee J, Laptenko O (2005) Bacterial transcription elongation factors: new insights into molecular mechanism of action. *Mol Microbiol* **55**(5): 1315-1324
- Borukhov S, Nudler E (2003) RNA polymerase holoenzyme: structure, function and biological implications. *Curr Opin Microbiol* **6**(2): 93-100
- Brieba LG, Gopal V, Sousa R (2001) Scanning mutagenesis reveals roles for helix n of the bacteriophage T7 RNA polymerase thumb subdomain in transcription complex stability, pausing, and termination. *J Biol Chem* **276**(13): 10306-10313.
- Brieba LG, Sousa R (2001a) T7 promoter release mediated by DNA scrunching. *Embo J* **20**(23): 6826-6835
- Brieba LG, Sousa R (2001b) The T7 RNA polymerase intercalating hairpin is important for promoter opening during initiation but not for RNA displacement or transcription bubble stability during elongation. *Biochemistry* **40**(13): 3882-3890.
- Cai H, Luse DS (1987) Variations in template protection by the RNA polymerase II transcription complex during the initiation process. *Mol Cell Biol* **7**(10): 3371-3379.
- Carpousis AJ, Gralla JD (1980) Cycling of ribonucleic acid polymerase to produce oligonucleotides during initiation in vitro at the lac UV5 promoter. *Biochemistry* **19**(14): 3245-3253
- Carpousis AJ, Gralla JD (1985) Interaction of RNA polymerase with lacUV5 promoter DNA during mRNA initiation and elongation. Footprinting, methylation, and rifampicin-sensitivity changes accompanying transcription initiation. *J Mol Biol* **183**(2): 165-177
- Cermakian N, Ikeda T, Cedergren R, Gray M (1996) Sequences homologous to yeast mitochondrial and bacteriophage T3 and T7 RNA polymerases are widespread throughout the eukaryotic lineage. *Nucleic Acids Res* **24**(4): 648-654
- Cheetham GM, Jeruzalmi D, Steitz TA (1999) Structural basis for initiation of transcription from an RNA polymerase- promoter complex. *Nature* **399**(6731): 80-83
- Cheetham GM, Steitz TA (1999) Structure of a transcribing T7 RNA polymerase initiation complex. *Science* **286**(5448): 2305-2309
- Clegg RM (1992) Fluorescence resonance energy transfer and nucleic acids. *Methods Enzymol* **211**: 353-388
- Diaz GA, Rong M, McAllister WT, Durbin RK (1996) The stability of abortively cycling T7 RNA polymerase complexes depends upon template conformation. *Biochemistry* **35**(33): 10837-10843

- dos Remedios CG, Moens PD (1995) Fluorescence resonance energy transfer spectroscopy is a reliable "ruler" for measuring structural changes in proteins. Dispelling the problem of the unknown orientation factor. *J Struct Biol* **115**(2): 175-185
- Dunn JJ, Studier FW (1983) Complete nucleotide sequence of bacteriophage T7 DNA and the locations of T7 genetic elements. *J Mol Biol* **166**(4): 477-535
- Ebright RH (2000) RNA polymerase: structural similarities between bacterial RNA polymerase and eukaryotic RNA polymerase II. *J Mol Biol* **304**(5): 687-698.
- Erlanson DA, Chytil M, Verdine GL (1996) The leucine zipper domain controls the orientation of AP-1 in the NFAT.AP-1.DNA complex. *Chem Biol* **3**(12): 981-991
- Esposito EA, Martin CT (2004a) Cross-linking of promoter DNA to T7 RNA polymerase does not prevent formation of a stable elongation complex. *J Biol Chem* **279**(43): 44270-44276
- Esposito EA, Martin CT (2004b) Crosslinking of promoter DNA to T7 RNA polymerase does not prevent formation of a stable elongation complex. *J Biol Chem* **279**(43): 44270-44276
- Gohlke C, Murchie AI, Lilley DM, Clegg RM (1994) Kinking of DNA and RNA helices by bulged nucleotides observed by fluorescence resonance energy transfer. *Proc Natl Acad Sci U S A* **91**(24): 11660-11664
- Gong P, Esposito EA, Martin CT (2004) Initial bubble collapse plays a key role in the transition to elongation in T7 RNA polymerase. *J Biol Chem* **279**(43): 44277-44285
- Gong P, Martin CT (2006) Mechanism of instability in abortive cycling by T7 RNA polymerase. *J Biol Chem* **281**(33): 23533-23544
- Gopal V, Brieba LG, Guajardo R, McAllister WT, Sousa R (1999) Characterization of Structural Features Important for T7 RNAP Elongation Complex Stability Reveals Competing Complex Conformations and a Role for the Non-template Strand in RNA Displacement. *J Mol Biol* **290**(2): 411-431
- Graham J, Cotton BA, Rong Xu, and Tom W. Muir (1999) Insertion of a Synthetic Peptide into a Recombinant Protein Framework: A Protein Biosensor. *J Am Chem Soc* **121**(5): 1100-1101
- Guillerez J, Lopez PJ, Proux F, Launay H, Dreyfus M (2005) A mutation in T7 RNA polymerase that facilitates promoter clearance. *Proc Natl Acad Sci U S A* **102**(17): 5958-5963

Guo Q, Nayak D, Brieba LG, Sousa R (2005) Major Conformational Changes During T7RNAP Transcription Initiation Coincide with, and are Required for, Promoter Release. *J Mol Biol*

Guo Q, Sousa R (2005a) Multiple roles for the T7 promoter nontemplate strand during transcription initiation and polymerase release. *J Biol Chem* **280**(5): 3474-3482

Guo Q, Sousa R (2005b) Weakening of the T7 promoter: Polymerase interaction facilitates promoter release. *J Biol Chem* **280**(15): 14956-14961

Hansen JL, Long AM, Schultz SC (1997) Structure of the RNA-dependent RNA polymerase of poliovirus. *Structure* **5**(8): 1109-1122

He B, Rong M, Durbin RK, McAllister WT (1997) A mutant T7 RNA polymerase that is defective in RNA binding and blocked in the early stages of transcription. *J Mol Biol* **265**(3): 275-288

Huang J, Sousa R (2000) T7 RNA Polymerase Elongation Complex Structure and Movement. *J Mol Biol* **303**(3): 347-358

Ikeda RA, Richardson CC (1986) Interactions of the RNA polymerase of bacteriophage T7 with its promoter during binding and initiation of transcription. *Proc Natl Acad Sci U S A* **83**(11): 3614-3618

Imburgio D, Rong M, Ma K, McAllister WT (2000) Studies of promoter recognition and start site selection by T7 RNA polymerase using a comprehensive collection of promoter variants. *Biochemistry* **39**(34): 10419-10430

Jaehning JA (1993) Mitochondrial transcription: is a pattern emerging? *Mol Microbiol* **8**(1): 1-4

Jeruzalmi D, Steitz TA (1998) Structure of T7 RNA polymerase complexed to the transcriptional inhibitor T7 lysozyme. *EMBO J* **17**(14): 4101-4113

Jia Y, Patel SS (1997) Kinetic mechanism of transcription initiation by bacteriophage T7 RNA polymerase. *Biochemistry* **36**(14): 4223-4232

Jiang M, Ma N, Vassilyev DG, McAllister WT (2004) RNA displacement and resolution of the transcription bubble during transcription by T7 RNA polymerase. *Mol Cell* **15**(5): 777-788

Jiang M, Rong M, Martin C, McAllister WT (2001) Interrupting the template strand of the T7 promoter facilitates translocation of the DNA during initiation, reducing transcript slippage and the release of abortive products. *J Mol Biol* **310**(3): 509-522.

- King GC, Martin CT, Pham TT, Coleman JE (1986) Transcription by T7 RNA polymerase is not zinc-dependent and is abolished on amidomethylation of cysteine-347. *Biochemistry* **25**(1): 36-40
- Klostermeier D, Millar DP (2001) Time-resolved fluorescence resonance energy transfer: a versatile tool for the analysis of nucleic acids. *Biopolymers* **61**(3): 159-179
- Kohlstaedt LA, Wang J, Friedman JM, Rice PA, Steitz TA (1992) Crystal structure at 3.5 Å resolution of HIV-1 reverse transcriptase complexed with an inhibitor. *Science* **256**(5065): 1783-1790
- Lescure B, Williamson V, Sentenac A (1981) Efficient and selective initiation by yeast RNA polymerase B in a dinucleotide-primed reaction. *Nucleic Acids Res* **9**(1): 31-45
- Ling ML, Risman SS, Klement JF, McGraw N, McAllister WT (1989) Abortive initiation by bacteriophage T3 and T7 RNA polymerases under conditions of limiting substrate [published erratum appears in *Nucleic Acids Res* 1989 Jun 12;17(11):4430]. *Nucleic Acids Res* **17**(4): 1605-1618
- Liu C, Martin CT (2001a) Fluorescence characterization of the transcription bubble in elongation complexes of T7 RNA polymerase. *J Mol Biol* **308**(3): 465-475.
- Liu C, Martin CT (2001b) Fluorescence characterization of the transcription bubble in elongation complexes of T7 RNA polymerase. *J Mol Biol* **308**(3): 465-475
- Liu C, Martin CT (2002) Promoter clearance by T7 RNA polymerase. Initial bubble collapse and transcript dissociation monitored by base analog fluorescence. *J Biol Chem* **277**(4): 2725-2731
- Lopez PJ, Guillerez J, Sousa R, Dreyfus M (1997) The low processivity of T7 RNA polymerase over the initially transcribed sequence can limit productive initiation in vivo. *J Mol Biol* **269**(1): 41-51
- Lorenz M, Hillisch A, Diekmann S (2002) Fluorescence resonance energy transfer studies of U-shaped DNA molecules. *J Biotechnol* **82**(3): 197-209
- Ma K, Temiakov D, Anikin M, McAllister WT (2005) Probing conformational changes in T7 RNA polymerase during initiation and termination by using engineered disulfide linkages. *Proc Natl Acad Sci U S A* **102**(49): 17612-17617
- Martin CT, Esposito EA, Theis K, Gong P (2005) Structure and Function in Promoter Escape by T7 RNA Polymerase. *Prog Nucl Acid Res Mol Biol* **80**: 323-347
- Martin CT, Muller DK, Coleman JE (1988) Processivity in early stages of transcription by T7 RNA polymerase. *Biochemistry* **27**(11): 3966-3974

McAllister WT (1993) Structure and function of the bacteriophage T7 RNA polymerase (or, the virtues of simplicity). *Cell Mol Biol Res* **39**(4): 385-391

McAllister WT (1997) Transcription by T7 RNA polymerase. *Nucleic Acids Mol Biol* **11**: 15–25

Mentesana PE, Chin-Bow ST, Sousa R, McAllister WT (2000) Characterization of Halted T7 RNA Polymerase Elongation Complexes Reveals Multiple Factors that Contribute to Stability. *J Mol Biol* **302**: 1049-1062

Milligan JF, Groebe DR, Witherell GW, Uhlenbeck OC (1987) Oligoribonucleotide synthesis using T7 RNA polymerase and synthetic DNA templates. *Nucleic Acids Res* **15**(21): 8783-8798

Moroney SE, Piccirilli JA (1991) Abortive products as initiating nucleotides during transcription by T7 RNA polymerase. *Biochemistry* **30**(42): 10343-10349

Muir TW, Sondhi D, Cole PA (1998) Expressed protein ligation: a general method for protein engineering. *Proc Natl Acad Sci U S A* **95**(12): 6705-6710

Mukherjee S, Brieba LG, Sousa R (2002) Structural transitions mediating transcription initiation by T7 RNA polymerase. *Cell* **110**(1): 81-91

Mukherjee S, Brieba LG, Sousa R (2003) Discontinuous movement and conformational change during pausing and termination by T7 RNA polymerase. *Embo J* **22**(24): 6483-6493

Muller DK, Martin CT, Coleman JE (1988) Processivity of proteolytically modified forms of T7 RNA polymerase. *Biochemistry* **27**(15): 5763-5771

Murakami KS, Darst SA (2003) Bacterial RNA polymerases: the whole story. *Curr Opin Struct Biol* **13**(1): 31-39

Muralidharan V, Muir TW (2006) Protein ligation: an enabling technology for the biophysical analysis of proteins. *Nat Methods* **3**(6): 429-438

Ota N, Hirano K, Warashina M, Andrus A, Mullah B, Hatanaka K, Taira K (1998) Determination of interactions between structured nucleic acids by fluorescence resonance energy transfer (FRET): selection of target sites for functional nucleic acids. *Nucleic Acids Res* **26**(3): 735-743

Parkhurst LJ, Parkhurst KM, Powell R, Wu J, Williams S (2001) Time-resolved fluorescence resonance energy transfer studies of DNA bending in double-stranded oligonucleotides and in DNA-protein complexes. *Biopolymers* **61**(3): 180-200

Place C, Oddos J, Buc H, McAllister WT, Buckle M (1999) Studies of contacts between T7 RNA polymerase and its promoter reveal features in common with multisubunit RNA polymerases. *Biochemistry* **38**(16): 4948-4957

Rong M, Durbin RK, McAllister WT (1998) Template strand switching by T7 RNA polymerase. *J Biol Chem* **273**(17): 10253-10260

Sapsford KE, Berti L, Medintz IL (2006) Materials for Fluorescence Resonance Energy Transfer Analysis: Beyond Traditional Donor-Acceptor Combinations. *Angew Chem Int Ed Engl* **45**(28): 4562-4589

Schick C, Martin CT (1993) Identification of specific contacts in T3 RNA polymerase-promoter interactions: kinetic analysis using small synthetic promoters. *Biochemistry* **32**(16): 4275-4280

Schroeder LA, deHaseth PL (2005) Mechanistic differences in promoter DNA melting by *Thermus aquaticus* and *Escherichia coli* RNA polymerases. *J Biol Chem* **280**(17): 17422-17429

Schultz LWaPG (2005) Expanding the Genetic Code. *Angew Chem Int Ed* **44**: 34-66

Song H, Kang C (2001) Sequence-specific termination by T7 RNA polymerase requires formation of paused conformation prior to the point of RNA release. *Genes Cells* **6**(4): 291-301.

Sousa R (2003) On models and methods for studying polymerase translocation. *Methods Enzymol* **371**: 3-13

Sousa R, Chung YJ, Rose JP, Wang BC (1993) Crystal structure of bacteriophage T7 RNA polymerase at 3.3 Å resolution. *Nature* **364**(6438): 593-599

Sousa R, Rose J, Wang B (1994) The thumb's knuckle. Flexibility in the thumb subdomain of T7 RNA polymerase is revealed by the structure of a chimeric T7/T3 RNA polymerase. *J Mol Biol* **244**(1): 6-12

Stano NM, Patel SS (2002) The intercalating beta-hairpin of T7 RNA polymerase plays a role in promoter DNA melting and in stabilizing the melted DNA for efficient RNA synthesis. *J Mol Biol* **315**(5): 1009-1025

Steitz TA (1999) DNA polymerases: structural diversity and common mechanisms. *J Biol Chem* **274**(25): 17395-17398

Straney DC, Crothers DM (1987a) Comparison of the open complexes formed by RNA polymerase at the *Escherichia coli* lac UV5 promoter. *J Mol Biol* **193**(2): 279-292

Straney DC, Crothers DM (1987b) A stressed intermediate in the formation of stably initiated RNA chains at the Escherichia coli lac UV5 promoter. *J Mol Biol* **193**(2): 267-278

Tahirov TH, Temiakov D, Anikin M, Patlan V, McAllister WT, Vassilyev DG, Yokoyama S (2002) Structure of a T7 RNA polymerase elongation complex at 2.9 Å resolution. *Nature* **420**(6911): 43-50

Tang GQ, Bandwar RP, Patel SS (2005) Extended upstream A-T sequence increases T7 promoter strength. *J Biol Chem* **280**(49): 40707-40713

Temiakov D, Montesana PE, Ma K, Mustaev A, Borukhov S, McAllister WT (2000) The specificity loop of T7 RNA polymerase interacts first with the promoter and then with the elongating transcript, suggesting a mechanism for promoter clearance. *Proc Natl Acad Sci U S A* **97**(26): 14109-14114

Temiakov D, Patlan V, Anikin M, McAllister WT, Yokoyama S, Vassilyev DG (2004) Structural basis for substrate selection by t7 RNA polymerase. *Cell* **116**(3): 381-391

Theis K, Gong P, Martin CT (2004) Topological and Conformational Analysis of the Initiation and Elongation Complex of T7 RNA Polymerase Suggests a New Twist. *Biochemistry* **43**(40): 12709-12715

Turingan RS, Liu C, Hawkins ME, Martin CT (2007a) Structural confirmation of a bent and open model for the initiation complex of T7 RNA polymerase. *Biochemistry* **46**(7): 1714-1723

Turingan RS, Theis K, Martin CT (2007b) Twisted or shifted? Fluorescence measurements of late intermediates in transcription initiation by T7 RNA polymerase. *Biochemistry* **46**(21): 6165-6168

Újvári A, Martin CT (1996) Thermodynamic and kinetic measurements of promoter binding by T7 RNA polymerase. *Biochemistry* **35**(46): 14574-14582

Wu P, Brand L (1994) Resonance energy transfer: methods and applications. *Anal Biochem* **218**(1): 1-13

Xu MQ, Perler FB (1996) The mechanism of protein splicing and its modulation by mutation. *EMBO J* **15**(19): 5146-5153

Yin YW, Steitz TA (2002) Structural basis for the transition from initiation to elongation transcription in T7 RNA polymerase. *Science* **298**(5597): 1387-1395

Yin YW, Steitz TA (2004) The structural mechanism of translocation and helicase activity in T7 RNA polymerase. *Cell* **116**(3): 393-404

BIBLIOGRAPHY

- Borukhov S, Lee J, Laptenko O (2005) Bacterial transcription elongation factors: new insights into molecular mechanism of action. *Mol Microbiol* **55**(5): 1315-1324
- Borukhov S, Nudler E (2003) RNA polymerase holoenzyme: structure, function and biological implications. *Curr Opin Microbiol* **6**(2): 93-100
- Brieba LG, Gopal V, Sousa R (2001) Scanning mutagenesis reveals roles for helix n of the bacteriophage T7 RNA polymerase thumb subdomain in transcription complex stability, pausing, and termination. *J Biol Chem* **276**(13): 10306-10313.
- Brieba LG, Sousa R (2001a) T7 promoter release mediated by DNA scrunching. *Embo J* **20**(23): 6826-6835
- Brieba LG, Sousa R (2001b) The T7 RNA polymerase intercalating hairpin is important for promoter opening during initiation but not for RNA displacement or transcription bubble stability during elongation. *Biochemistry* **40**(13): 3882-3890.
- Cai H, Luse DS (1987) Variations in template protection by the RNA polymerase II transcription complex during the initiation process. *Mol Cell Biol* **7**(10): 3371-3379.
- Carpousis AJ, Gralla JD (1980) Cycling of ribonucleic acid polymerase to produce oligonucleotides during initiation in vitro at the lac UV5 promoter. *Biochemistry* **19**(14): 3245-3253
- Carpousis AJ, Gralla JD (1985) Interaction of RNA polymerase with lacUV5 promoter DNA during mRNA initiation and elongation. Footprinting, methylation, and rifampicin-sensitivity changes accompanying transcription initiation. *J Mol Biol* **183**(2): 165-177
- Cermakian N, Ikeda T, Cedergren R, Gray M (1996) Sequences homologous to yeast mitochondrial and bacteriophage T3 and T7 RNA polymerases are widespread throughout the eukaryotic lineage. *Nucleic Acids Res* **24**(4): 648-654
- Cheetham GM, Jeruzalmi D, Steitz TA (1999) Structural basis for initiation of transcription from an RNA polymerase- promoter complex. *Nature* **399**(6731): 80-83
- Cheetham GM, Steitz TA (1999) Structure of a transcribing T7 RNA polymerase initiation complex. *Science* **286**(5448): 2305-2309
- Clegg RM (1992) Fluorescence resonance energy transfer and nucleic acids. *Methods Enzymol* **211**: 353-388
- Diaz GA, Rong M, McAllister WT, Durbin RK (1996) The stability of abortively cycling T7 RNA polymerase complexes depends upon template conformation. *Biochemistry* **35**(33): 10837-10843

- dos Remedios CG, Moens PD (1995) Fluorescence resonance energy transfer spectroscopy is a reliable "ruler" for measuring structural changes in proteins. Dispelling the problem of the unknown orientation factor. *J Struct Biol* **115**(2): 175-185
- Dunn JJ, Studier FW (1983) Complete nucleotide sequence of bacteriophage T7 DNA and the locations of T7 genetic elements. *J Mol Biol* **166**(4): 477-535
- Ebright RH (2000) RNA polymerase: structural similarities between bacterial RNA polymerase and eukaryotic RNA polymerase II. *J Mol Biol* **304**(5): 687-698.
- Erlanson DA, Chytil M, Verdine GL (1996) The leucine zipper domain controls the orientation of AP-1 in the NFAT.AP-1.DNA complex. *Chem Biol* **3**(12): 981-991
- Esposito EA, Martin CT (2004a) Cross-linking of promoter DNA to T7 RNA polymerase does not prevent formation of a stable elongation complex. *J Biol Chem* **279**(43): 44270-44276
- Esposito EA, Martin CT (2004b) Crosslinking of promoter DNA to T7 RNA polymerase does not prevent formation of a stable elongation complex. *J Biol Chem* **279**(43): 44270-44276
- Gohlke C, Murchie AI, Lilley DM, Clegg RM (1994) Kinking of DNA and RNA helices by bulged nucleotides observed by fluorescence resonance energy transfer. *Proc Natl Acad Sci U S A* **91**(24): 11660-11664
- Gong P, Esposito EA, Martin CT (2004) Initial bubble collapse plays a key role in the transition to elongation in T7 RNA polymerase. *J Biol Chem* **279**(43): 44277-44285
- Gong P, Martin CT (2006) Mechanism of instability in abortive cycling by T7 RNA polymerase. *J Biol Chem* **281**(33): 23533-23544
- Gopal V, Brieba LG, Guajardo R, McAllister WT, Sousa R (1999) Characterization of Structural Features Important for T7 RNAP Elongation Complex Stability Reveals Competing Complex Conformations and a Role for the Non-template Strand in RNA Displacement. *J Mol Biol* **290**(2): 411-431
- Graham J, Cotton BA, Rong Xu, and Tom W. Muir (1999) Insertion of a Synthetic Peptide into a Recombinant Protein Framework: A Protein Biosensor. *J Am Chem Soc* **121**(5): 1100-1101
- Guillerez J, Lopez PJ, Proux F, Launay H, Dreyfus M (2005) A mutation in T7 RNA polymerase that facilitates promoter clearance. *Proc Natl Acad Sci U S A* **102**(17): 5958-5963

Guo Q, Nayak D, Brieba LG, Sousa R (2005) Major Conformational Changes During T7RNAP Transcription Initiation Coincide with, and are Required for, Promoter Release. *J Mol Biol*

Guo Q, Sousa R (2005a) Multiple roles for the T7 promoter nontemplate strand during transcription initiation and polymerase release. *J Biol Chem* **280**(5): 3474-3482

Guo Q, Sousa R (2005b) Weakening of the T7 promoter: Polymerase interaction facilitates promoter release. *J Biol Chem* **280**(15): 14956-14961

Hansen JL, Long AM, Schultz SC (1997) Structure of the RNA-dependent RNA polymerase of poliovirus. *Structure* **5**(8): 1109-1122

He B, Rong M, Durbin RK, McAllister WT (1997) A mutant T7 RNA polymerase that is defective in RNA binding and blocked in the early stages of transcription. *J Mol Biol* **265**(3): 275-288

Huang J, Sousa R (2000) T7 RNA Polymerase Elongation Complex Structure and Movement. *J Mol Biol* **303**(3): 347-358

Ikeda RA, Richardson CC (1986) Interactions of the RNA polymerase of bacteriophage T7 with its promoter during binding and initiation of transcription. *Proc Natl Acad Sci U S A* **83**(11): 3614-3618

Imburgio D, Rong M, Ma K, McAllister WT (2000) Studies of promoter recognition and start site selection by T7 RNA polymerase using a comprehensive collection of promoter variants. *Biochemistry* **39**(34): 10419-10430

Jaehning JA (1993) Mitochondrial transcription: is a pattern emerging? *Mol Microbiol* **8**(1): 1-4

Jeruzalmi D, Steitz TA (1998) Structure of T7 RNA polymerase complexed to the transcriptional inhibitor T7 lysozyme. *EMBO J* **17**(14): 4101-4113

Jia Y, Patel SS (1997) Kinetic mechanism of transcription initiation by bacteriophage T7 RNA polymerase. *Biochemistry* **36**(14): 4223-4232

Jiang M, Ma N, Vassilyev DG, McAllister WT (2004) RNA displacement and resolution of the transcription bubble during transcription by T7 RNA polymerase. *Mol Cell* **15**(5): 777-788

Jiang M, Rong M, Martin C, McAllister WT (2001) Interrupting the template strand of the T7 promoter facilitates translocation of the DNA during initiation, reducing transcript slippage and the release of abortive products. *J Mol Biol* **310**(3): 509-522.

- King GC, Martin CT, Pham TT, Coleman JE (1986) Transcription by T7 RNA polymerase is not zinc-dependent and is abolished on amidomethylation of cysteine-347. *Biochemistry* **25**(1): 36-40
- Klostermeier D, Millar DP (2001) Time-resolved fluorescence resonance energy transfer: a versatile tool for the analysis of nucleic acids. *Biopolymers* **61**(3): 159-179
- Kohlstaedt LA, Wang J, Friedman JM, Rice PA, Steitz TA (1992) Crystal structure at 3.5 Å resolution of HIV-1 reverse transcriptase complexed with an inhibitor. *Science* **256**(5065): 1783-1790
- Lescure B, Williamson V, Sentenac A (1981) Efficient and selective initiation by yeast RNA polymerase B in a dinucleotide-primed reaction. *Nucleic Acids Res* **9**(1): 31-45
- Ling ML, Risman SS, Klement JF, McGraw N, McAllister WT (1989) Abortive initiation by bacteriophage T3 and T7 RNA polymerases under conditions of limiting substrate [published erratum appears in *Nucleic Acids Res* 1989 Jun 12;17(11):4430]. *Nucleic Acids Res* **17**(4): 1605-1618
- Liu C, Martin CT (2001a) Fluorescence characterization of the transcription bubble in elongation complexes of T7 RNA polymerase. *J Mol Biol* **308**(3): 465-475
- Liu C, Martin CT (2001b) Fluorescence characterization of the transcription bubble in elongation complexes of T7 RNA polymerase. *J Mol Biol* **308**(3): 465-475.
- Liu C, Martin CT (2002) Promoter clearance by T7 RNA polymerase. Initial bubble collapse and transcript dissociation monitored by base analog fluorescence. *J Biol Chem* **277**(4): 2725-2731
- Lopez PJ, Guillerez J, Sousa R, Dreyfus M (1997) The low processivity of T7 RNA polymerase over the initially transcribed sequence can limit productive initiation in vivo. *J Mol Biol* **269**(1): 41-51
- Lorenz M, Hillisch A, Diekmann S (2002) Fluorescence resonance energy transfer studies of U-shaped DNA molecules. *J Biotechnol* **82**(3): 197-209
- Ma K, Temiakov D, Anikin M, McAllister WT (2005) Probing conformational changes in T7 RNA polymerase during initiation and termination by using engineered disulfide linkages. *Proc Natl Acad Sci U S A* **102**(49): 17612-17617
- Martin CT, Esposito EA, Theis K, Gong P (2005) Structure and Function in Promoter Escape by T7 RNA Polymerase. *Prog Nucl Acid Res Mol Biol* **80**: 323-347
- Martin CT, Muller DK, Coleman JE (1988) Processivity in early stages of transcription by T7 RNA polymerase. *Biochemistry* **27**(11): 3966-3974

McAllister WT (1993) Structure and function of the bacteriophage T7 RNA polymerase (or, the virtues of simplicity). *Cell Mol Biol Res* **39**(4): 385-391

McAllister WT (1997) Transcription by T7 RNA polymerase. *Nucleic Acids Mol Biol* **11**: 15–25

Mentesana PE, Chin-Bow ST, Sousa R, McAllister WT (2000) Characterization of Halted T7 RNA Polymerase Elongation Complexes Reveals Multiple Factors that Contribute to Stability. *J Mol Biol* **302**: 1049-1062

Milligan JF, Groebe DR, Witherell GW, Uhlenbeck OC (1987) Oligoribonucleotide synthesis using T7 RNA polymerase and synthetic DNA templates. *Nucleic Acids Res* **15**(21): 8783-8798

Moroney SE, Piccirilli JA (1991) Abortive products as initiating nucleotides during transcription by T7 RNA polymerase. *Biochemistry* **30**(42): 10343-10349

Muir TW, Sondhi D, Cole PA (1998) Expressed protein ligation: a general method for protein engineering. *Proc Natl Acad Sci U S A* **95**(12): 6705-6710

Mukherjee S, Brieba LG, Sousa R (2002) Structural transitions mediating transcription initiation by T7 RNA polymerase. *Cell* **110**(1): 81-91

Mukherjee S, Brieba LG, Sousa R (2003) Discontinuous movement and conformational change during pausing and termination by T7 RNA polymerase. *Embo J* **22**(24): 6483-6493

Muller DK, Martin CT, Coleman JE (1988) Processivity of proteolytically modified forms of T7 RNA polymerase. *Biochemistry* **27**(15): 5763-5771

Murakami KS, Darst SA (2003) Bacterial RNA polymerases: the whole story. *Curr Opin Struct Biol* **13**(1): 31-39

Muralidharan V, Muir TW (2006) Protein ligation: an enabling technology for the biophysical analysis of proteins. *Nat Methods* **3**(6): 429-438

Ota N, Hirano K, Warashina M, Andrus A, Mullah B, Hatanaka K, Taira K (1998) Determination of interactions between structured nucleic acids by fluorescence resonance energy transfer (FRET): selection of target sites for functional nucleic acids. *Nucleic Acids Res* **26**(3): 735-743

Parkhurst LJ, Parkhurst KM, Powell R, Wu J, Williams S (2001) Time-resolved fluorescence resonance energy transfer studies of DNA bending in double-stranded oligonucleotides and in DNA-protein complexes. *Biopolymers* **61**(3): 180-200

Place C, Oddos J, Buc H, McAllister WT, Buckle M (1999) Studies of contacts between T7 RNA polymerase and its promoter reveal features in common with multisubunit RNA polymerases. *Biochemistry* **38**(16): 4948-4957

Rong M, Durbin RK, McAllister WT (1998) Template strand switching by T7 RNA polymerase. *J Biol Chem* **273**(17): 10253-10260

Sapsford KE, Berti L, Medintz IL (2006) Materials for Fluorescence Resonance Energy Transfer Analysis: Beyond Traditional Donor-Acceptor Combinations. *Angew Chem Int Ed Engl* **45**(28): 4562-4589

Schick C, Martin CT (1993) Identification of specific contacts in T3 RNA polymerase-promoter interactions: kinetic analysis using small synthetic promoters. *Biochemistry* **32**(16): 4275-4280

Schroeder LA, deHaseth PL (2005) Mechanistic differences in promoter DNA melting by *Thermus aquaticus* and *Escherichia coli* RNA polymerases. *J Biol Chem* **280**(17): 17422-17429

Schultz LWaPG (2005) Expanding the Genetic Code. *Angew Chem Int Ed* **44**: 34-66

Song H, Kang C (2001) Sequence-specific termination by T7 RNA polymerase requires formation of paused conformation prior to the point of RNA release. *Genes Cells* **6**(4): 291-301.

Sousa R (2003) On models and methods for studying polymerase translocation. *Methods Enzymol* **371**: 3-13

Sousa R, Chung YJ, Rose JP, Wang BC (1993) Crystal structure of bacteriophage T7 RNA polymerase at 3.3 Å resolution. *Nature* **364**(6438): 593-599

Sousa R, Rose J, Wang B (1994) The thumb's knuckle. Flexibility in the thumb subdomain of T7 RNA polymerase is revealed by the structure of a chimeric T7/T3 RNA polymerase. *J Mol Biol* **244**(1): 6-12

Stano NM, Patel SS (2002) The intercalating beta-hairpin of T7 RNA polymerase plays a role in promoter DNA melting and in stabilizing the melted DNA for efficient RNA synthesis. *J Mol Biol* **315**(5): 1009-1025

Steitz TA (1999) DNA polymerases: structural diversity and common mechanisms. *J Biol Chem* **274**(25): 17395-17398

Straney DC, Crothers DM (1987a) A stressed intermediate in the formation of stably initiated RNA chains at the *Escherichia coli* lac UV5 promoter. *J Mol Biol* **193**(2): 267-278

- Straney DC, Crothers DM (1987b) Comparison of the open complexes formed by RNA polymerase at the Escherichia coli lac UV5 promoter. *J Mol Biol* **193**(2): 279-292
- Tahirov TH, Temiakov D, Anikin M, Patlan V, McAllister WT, Vassylyev DG, Yokoyama S (2002) Structure of a T7 RNA polymerase elongation complex at 2.9 Å resolution. *Nature* **420**(6911): 43-50
- Tang GQ, Bandwar RP, Patel SS (2005) Extended upstream A-T sequence increases T7 promoter strength. *J Biol Chem* **280**(49): 40707-40713
- Temiakov D, Montesana PE, Ma K, Mustaev A, Borukhov S, McAllister WT (2000) The specificity loop of T7 RNA polymerase interacts first with the promoter and then with the elongating transcript, suggesting a mechanism for promoter clearance. *Proc Natl Acad Sci U S A* **97**(26): 14109-14114
- Temiakov D, Patlan V, Anikin M, McAllister WT, Yokoyama S, Vassylyev DG (2004) Structural basis for substrate selection by t7 RNA polymerase. *Cell* **116**(3): 381-391
- Theis K, Gong P, Martin CT (2004) Topological and Conformational Analysis of the Initiation and Elongation Complex of T7 RNA Polymerase Suggests a New Twist. *Biochemistry* **43**(40): 12709-12715
- Turingan RS, Liu C, Hawkins ME, Martin CT (2007a) Structural confirmation of a bent and open model for the initiation complex of T7 RNA polymerase. *Biochemistry* **46**(7): 1714-1723
- Turingan RS, Theis K, Martin CT (2007b) Twisted or shifted? Fluorescence measurements of late intermediates in transcription initiation by T7 RNA polymerase. *Biochemistry* **46**(21): 6165-6168
- Újvári A, Martin CT (1996) Thermodynamic and kinetic measurements of promoter binding by T7 RNA polymerase. *Biochemistry* **35**(46): 14574-14582
- Wu P, Brand L (1994) Resonance energy transfer: methods and applications. *Anal Biochem* **218**(1): 1-13
- Xu MQ, Perler FB (1996) The mechanism of protein splicing and its modulation by mutation. *EMBO J* **15**(19): 5146-5153
- Yin YW, Steitz TA (2002) Structural basis for the transition from initiation to elongation transcription in T7 RNA polymerase. *Science* **298**(5597): 1387-1395
- Yin YW, Steitz TA (2004) The structural mechanism of translocation and helicase activity in T7 RNA polymerase. *Cell* **116**(3): 393-404